increases slowly with wavelength, passes through a maximum, and falls rapidly at the longer wavelengths. The wavelength at which the sensitivity becomes half of the maximum value is 3.8 μ. This value corresponds to an energy of 0.33 eV which is in good agreement with the value obtained by measuring the absorption coefficient. Curves 2 and 3 are the quantum efficiency of the PEM effect for light polarized perpendicular and parallel to the c axis of the crystal. Comparing these curves, it will be seen that the wavelength $\lambda(\frac{1}{2})$ at which the sensitivity becomes a half of the maximum value is 3.4 μ in curve 3 and 3.7 μ in curve 2. The discrepancy between the two curves is interpreted as the result of the anisotropy of the crystal structure of tellurium. This interpretation is supported by observations of the absorption coefficient of tellurium.[6]

[6] J. J. Loferski, Phys. Rev. **93**, 707 (1954).

PHYSICAL REVIEW VOLUME 135, NUMBER 6A 14 SEPTEMBER 1964

Lattice Sum Evaluations of Ruby Spectral Parameters*

J. O. ARTMAN AND JOHN C. MURPHY
Applied Physics Laboratory, The Johns Hopkins University, Silver Spring, Maryland
(Received 4 March 1964; revised manuscript received 15 April 1964)

This paper presents the results of an attempt to collate many of the known spectroscopic properties of ruby in the strong field coupling scheme within the framework of an ionic model. The Tanabe-Sugano theory extended to odd symmetry crystal fields is used in this analysis. The appropriate Madelung and higher order potentials are computed for both a point-ion and a point-dipolar lattice. The radius of convergence of these sums found with our procedure is much smaller than those reported by McClure and others. The lattice potentials derived from a particular model of the Cr^{3+} local environment give a reasonable fit to many of the measurable spectroscopic parameters. In addition to the conventional optical splittings, these include optical intensities, pressure and "electric field" effects. The interpretation of the Cr^{53} nuclear electric quadrupole moment is shown to be sensitive to the details of the Cr^{3+} environment. Some results are given for other ions and also for Al^{3+} in corundum.

INTRODUCTION

THE general procedure that will be followed in this paper is to assume the so-called crystal-field theory in its most general form. Here the form of the tensor operators is determined by the symmetry of the site under consideration and the tensor coefficients are determined from experiment. It follows that within the framework of the theory relations exist between quite diverse experimental parameters which depend only on the symmetry of the site under consideration. Subsequently, an "ionic" model for the interactions in the corundum lattice will be introduced which will be used to evaluate many of these potential coefficients explicitly by the method of lattice sums. This approximation to the actual interactions in a crystal clearly is quite crude in comparison to a complete molecular-orbital treatment. However, carrying out this latter program leads to conceptual and computational difficulties. Those calculations which have actually been made to date required approximations whose validity is uncertain. Covalency effects have been introduced, for example, via a limited number of adjustable parameters such as the Koide-Pryce ϵ or the ionization potential of the ions in the crystal; interactions with the rest of the lattice were ignored despite the long-range character of the Coulomb interaction.[1-3] In such a situation the actual usefulness of the separate approximations probably depends on what experimental aspects of the problem are under consideration.

Recently, Sugano and Shulman[4] performed a complete molecular orbital calculation on the $(NiF_6)^{4-}$ complex in $KMnF_3$ neglecting the rest of the lattice and have obtained good agreement with experiment. If we leave aside some recent criticism[4] of their molecular orbital procedure, their calculations would indicate that a large degree of covalency is required for this structure. They justify the neglect of extracomplex interactions by showing that the potential field of the entire lattice outside of the complex under consideration evaluated at the nuclear position of each member of the complex is approximately constant. (The variation of this "reduced" Madelung potential evaluated at Ni and F sites is 0.26 eV.) The complex is thus immersed in a field of constant potential and to a first approximation

* This work supported by the Bureau of Naval Weapons, U. S. Department of the Navy, under Contract NOw 62-0604-c.

[1] S. Koide and M. H. L. Pryce, Phil. Mag. **3**, 607 (1958).
[2] S. Sugano and M. Peter, Phys. Rev. **122**, 381 (1961).
[3] L. L. Lohr, Jr., and W. N. Lipscomb, J. Chem. Phys. **38**, 1607 (1963).
[4] R. G. Shulman and S. Sugano, Phys. Rev. **130**, 506 (1963); K. Knox, R. G. Shulman, and S. Sugano, Phys. Rev. **130**, 512 (1963); S. Sugano and R. G. Shulman, Phys. Rev. **130**, 517 (1963). But see a recent criticism by R. E. Watson and A. J. Freeman, Phys. Rev. **134**, A1526 (1964) of the molecular orbital treatment employed in this work.

TABLE I. Atomic positions and lattice parameters for corundum-type structures. Hexagonal coordinates. Space group D_{3d}^6.[a]

Metal ion:
$$\left\{\begin{array}{ccc} a & b & c \\ 0 & 0 & w \\ 0 & 0 & -w \\ 0 & 0 & \frac{1}{2}+w \\ 0 & 0 & \frac{1}{2}-w \end{array}\right\}+\left\{\begin{array}{ccc} 0 & 0 & 0 \\ \frac{1}{3} & \frac{2}{3} & \frac{2}{3} \\ \frac{2}{3} & \frac{1}{3} & \frac{1}{3} \end{array}\right\}+hkl$$

Oxygen:
$$\left\{\begin{array}{ccc} v & 0 & 0 \\ -v & -v & 0 \\ 0 & v & 0 \\ -v & 0 & \frac{1}{2} \\ v & v & \frac{1}{2} \\ 0 & -v & \frac{1}{2} \end{array}\right\}+\left\{\begin{array}{ccc} 0 & 0 & 0 \\ \frac{1}{3} & \frac{2}{3} & \frac{2}{3} \\ \frac{2}{3} & \frac{1}{3} & \frac{1}{3} \end{array}\right\}+hkl$$

	$\alpha-Al_2O_3$	Ti_2O_3	V_2O_3	Cr_2O_3	$\alpha-Fe_2O_3$
A_0 (Å)	4.7589	5.149	4.952	4.9607	5.0345
C_0 (Å)	12.991	13.642	14.002	13.599	13.749
w	0.1020	0.0950	0.0963	0.0975	0.105
v	0.306	0.317	0.315	0.306	0.300

[a] Adapted from R. E. Newnham and Y. M. De Haan, Z. Krist. 117, 235 (1962).

is independent of the rest of the lattice. Direct extension of the results of this paper to the substituted Al_2O_3 system is clouded by at least two considerations. On one hand, our calculation of the Madelung potential arising from all atoms outside the primary $(CrO_6)^{9-}$ complex indicates a variation of the Madelung potential one order of magnitude larger than the case considered in Ref. 4. The actual variation (4.1 eV) is of the same order of magnitude as the optical energy differences. Moreover, unlike the situation in $K(Ni)MnF_3$, the Cr and O ions in ruby are *not* at centers of inversion. The electric fields across the $(CrO_6)^{9-}$ complex thus are large and rapidly varying.

In this paper it will be shown that application of the so-called "ionic" model can correlate consistently many aspects of the corundum spectral system. Stress and electric effects in particular play a prominent role in our analysis. In addition, based on the particular model which we have chosen for the local crystal environment,

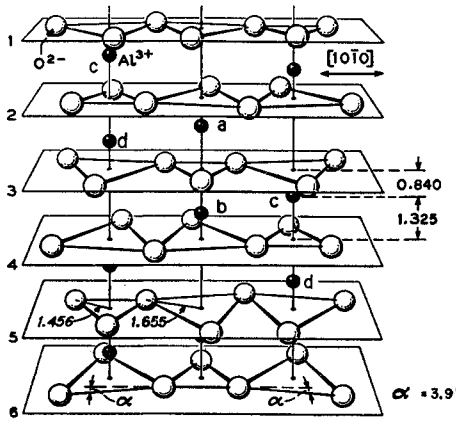

FIG. 1. The corundum lattice.

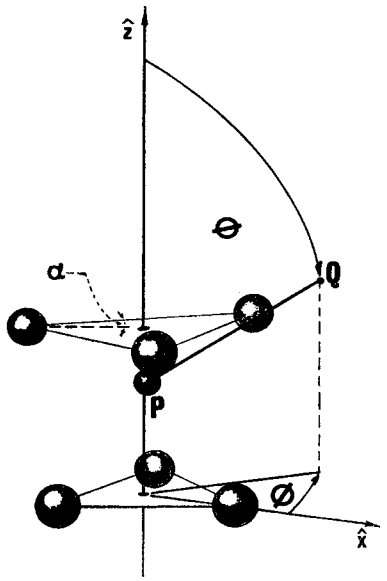

FIG. 2. The six nearest oxygen neighbors about an aluminum on a type (c) site. The coordinate system used in the lattice sum computations is also indicated.

there are certain new results which may provide independent confirmation of this approach.

LATTICE GEOMETRY

The corundum lattice is shown in Fig. 1.[5] The space group is D_{3d}^6 or equivalently $R\bar{3}c$. The Al site symmetry is C_3. There are four types of nonequivalent Al sites in the corundum structure which we denote as (a), (b), (c), and (d). A tabulation of the atomic positions and lattice parameters for corundum-type structures, taken from Newnham and de Haan,[6] is presented in Table I. The unit cell is composed of 12 Al ions and 18 O ions—thus each type of Al site occurs three times.

The nearest neighbors of an Al, on a type (c) site for example, are indicated in Fig. 2. The three upper oxygens lie on the vertices of a triangle which is skewed by the angle α with respect to the smaller triangle formed by three lower oxygen ions. The Al is closer to the plane of the upper oxygens. The selection of an

TABLE II. Monopolar potential constants.

1. $B_0^0=e/R$
2. $B_1^0=(e/R^2)\cos\theta$
3. $B_2^0=(e/4R^3)(3\cos^2\theta-1)$
4. $B_3^0=(e/4R^4)(5\cos^3\theta-3\cos\theta)$
5. $B_3^3=(5e/8R^4)\sin^3\theta\cos3\varphi$
6. $C_3^3=(5e/8R^4)\sin^3\theta\sin3\varphi$
7. $B_4^0=(e/64R^5)(35\cos^4\theta-30\cos^2\theta+3)$
8. $B_4^3=(70e/16R^5)\sin^3\theta\cos\theta\cos3\varphi$
9. $C_4^3=(70e/16R^5)\sin^3\theta\cos\theta\sin^3\varphi$

[5] Adapted from S. Geschwind and J. P. Remeika, Phys. Rev. 122, 757 (1961).
[6] R. E. Newnham and Y. M. De Haan, Z. Krist. 117, 235 (1962).

TABLE III. Relative signs of the lattice potential constants for the four nonequivalent types of Al^{3+} sites in corundum.

Lattice site	Potential constants B_0^0	B_1^0	B_2^0	B_3^0	B_3^3	C_3^3	B_4^0	B_4^3	C_4^3
(c)	+	+	+	+	+	+	+	+	+
(a)	+	+	+	+	+	−	+	+	−
(d)	+	−	+	−	−	+	+	+	−
(b)	+	−	+	−	−	−	+	+	+

appropriate coordinate system in which to calculate the lattice potential components is dictated by crystal geometry. A conventional xyz system is referenced to axes derived from the "nontwisted" oxygen triangle and the c-axis direction, as shown in Fig. 2. The co-latitude θ and longitude φ are defined in the standard fashion.

Since an Al site possesses C_3 symmetry, the non-vanishing elements of the potential evaluated at such a reference correspond to those spherical harmonics Y_l^m for which $m=0, \pm 3$. Both even and odd values of l are permitted. If an impurity ion such as Cr^{3+} occupied an Al site, a potential function V sufficiently general to describe the properties of a d electron can be written in the form[7]

$$V=B_0^0+B_1^0 r\cos\theta+B_2^0 r^2(3\cos^2\theta-1)$$
$$+B_3^0 r^3(5\cos^3\theta-3\cos\theta)+B_3^3 r^3\sin^3\theta\cos 3\varphi$$
$$+C_3^3 r^3\sin^3\theta\sin 3\varphi+B_4^0 r^4(35\cos^4\theta-30\cos^2\theta+3)$$
$$+B_4^3 r^4\sin^3\theta\cos\theta\cos 3\varphi+C_4^3 r^4\sin^3\theta\cos\theta\sin 3\varphi.$$

The B and C potential constants are found by summation over the entire lattice. The forms of these terms are indicated in Table II. To be consistent, the coordinate system used to evaluate the lattice sums at sites (a), (b), and (d) *must* be the same as that used for site (c). The absolute values of the various respective sums at all the four sites are the same. However, the relative algebraic signs conform to the dictates of crystal geometry; this is illustrated in Table III.

A tabulation of the potential constants at a type (c) site is given in Table IV. The units used, as given by McClure,[7] are convenient when discussing optical energy differences. (Henceforth, all references to "McClure" without additional specification will denote Ref. 7.) The values are given for summations over the ions enveloped by spheres of radii 1, 2, 3, and $4A_0$. The nearest-neighbor results are also listed for comparison. The algebraic signs in Table IV differ somewhat from those of McClure's computation. (The present results are consistent with the coordinate system of Fig. 2 and the requirements of group theory.) McClure also seems to have missed the reversal in sign of C_3^3 in going from nearest neighbors to larger sphere radii and to have obtained too large a value for C_4^3. It will be noted that the convergence of some of the terms, particularly B_0^0 and B_1^0, is rather poor.

Nijboer and deWette[8] have advanced a more rapidly convergent lattice sum procedure involving in part summation over the inverse lattice. Their procedure unfortunately usually is not convergent for inverse powers of R less than 4. Wood[9] developed a method for the calculation of Madelung constants in crystals of low symmetry which we have adapted to our case. The ions are grouped into "molecules" of zero electrical charge; the summation then proceeds over arrays of "molecules." This procedure allows the presence of surface (deBoer) effects to be ignored. Wood in his examples found that the rapidity of convergence depended upon the method used to group the cells. Grouping by shells or layers about the central cell containing the reference ion was more effective than grouping the cells according to their contributions to the energy!

The simplest obvious choice for the "molecule" is just an "Al_2O_3" assembly. Each such assembly consists of a small nontwisted triangle of oxygens with

TABLE IV. Potential constants for type (c) Al site in corundum. Summation over ions contained within spheres of various radii. Units of eV per unit charge on the O^{2-} ion per $Å^n$.

	nn 6 O	$R=A_0$ 20 Al, 36 O	$R=2A_0$ 170 Al, 243 O	$R=3A_0$ 533 Al, 819 O	$R=4A_0$ 1336 Al, 1962 O
1. B_0^0	45.21102	32.14761	−3.43295	37.48354	−16.13113
2. B_1^0	−1.82516	−1.86236	−0.21953	0.34123	0.45744
3. B_2^0	−0.14307	−0.03310	−0.17629	−0.20587	−0.14806
4. B_3^0	−0.45787	−0.29627	−0.30065	−0.30116	−0.30159
5. B_3^3	−0.85202	−0.76468	−0.75950	−0.76118	−0.76100
6. C_3^3	−0.32729	0.05198	0.03826	0.04696	0.04255
7. B_4^0	−0.12910	−0.14388	−0.14339	−0.14331	−0.14332
8. B_4^3	−4.43451	−4.26653	−4.23848	−4.23628	−4.23647
9. C_4^3	−0.47883	−0.67815	−0.68994	−0.68992	−0.68993

[7] D. S. McClure, J. Chem. Phys. **36**, 2757 (1962).
[8] B. R. A. Nijboer and F. W. deWette, Physica **23**, 309 (1957).
[9] R. H. Wood, J. Chem. Phys. **32**, 1690 (1960).

TABLE V. Potential constants for type (c) Al site in corundum. Summation over clusters contained within spheres of various radii as explained in text. "Madelung" method.

	$R=A_0$ 13 cells	$R=2A_0$ 87 cells	$R=3A_0$ 284 cells	$R=4A_0$ 683 cells
1. B_0^0	19.74356	17.39315	17.26653	17.37943
2. B_1^0	−0.23007	0.36301	0.40182	0.40966
3. B_2^0	−0.39942	−0.15969	−0.15136	−0.15149
4. B_3^0	−0.40187	−0.30185	−0.30203	−0.30194
5. B_3^3	−0.75008	−0.76141	−0.76161	−0.76164
6. C_3^3	0.22458	0.04463	0.04422	0.04428
7. B_4^0	−0.14759	−0.14333	−0.14334	−0.14333
8. B_4^3	−4.25001	−4.23647	−4.23655	−4.23652
9. C_4^3	−0.48072	−0.68941	−0.68991	−0.68989

aluminums immediately above and below. There are two types of such hexahedra (bypyramids). One type consists of an oxygen triangle with a type (a, b) aluminum pair, the other an oxygen triangle with a (c, d) aluminum pair. The Bravais unit cell is composed of three each such bipyramids. Figure 3 shows a view of a (c, d) bipyramid in the foreground with the three nearest upper (a, b) bipyramids disposed about it.

Table V is a tabulation similar to that of Table IV carried out by the Madelung cell method. Contributions from bipyramids whose *centroids* are on or within spheres of radii 1, 2, 3, and $4A_0$, respectively, were considered. The convergence difficulties encountered in the previous tabulation of B_0^0 and B_1^0 are eliminated. Table V suggests that a "sphere of influence" of radius $2A_0$ containing 87 cells (435 ions) is necessary to obtain reasonably good convergence of all the potential terms. In view of the remarks made by Wood, we attempted to see whether we could establish a smaller "zone of influence," not necessarily spherical in shape. Since it is extremely difficult to visualize the geometrical details, Fig. 4 and accompanying Table VI were prepared. Figure 4 shows the locations of the bipyramid centroids

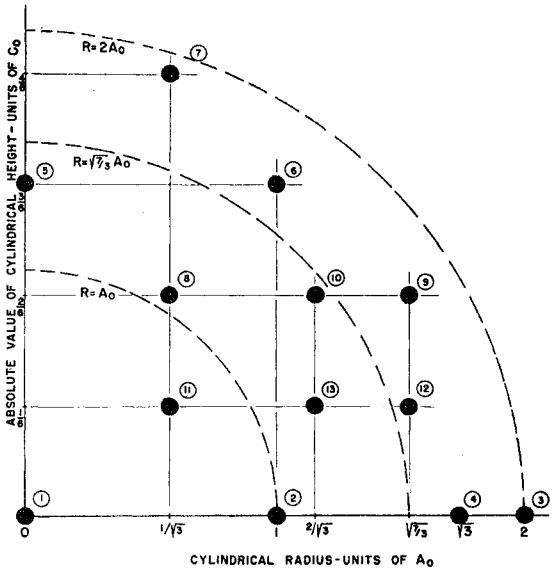

FIG. 4. Locations of Al_2O_3 bipyramid centroids contained on or within a sphere of radius $2A_0$. Absolute values of the cylindrical coordinates are employed. Refer to Table VI for the number and type of the bipyramids at each location.

contained on or within a sphere of radius $2A_0$ in compact form. When specified in terms of the cylindrical radius and the absolute value of the cylindrical height, there are 13 such clusters. The breakdown of the number of cells per cluster and the bipyramid designations are given in Table VI. The summations over various combinations of these clusters are given in Table VII. It appears that when summing by *this technique* we can educe the "zone of influence" about an Al to a rough sphere of radius $\sim(7/3)^{1/2}A_0$ containing 33 cells (165 ions).

As a result of the above development we are in a position to recompute the Madelung constant M of corundum. The only existing value in the literature

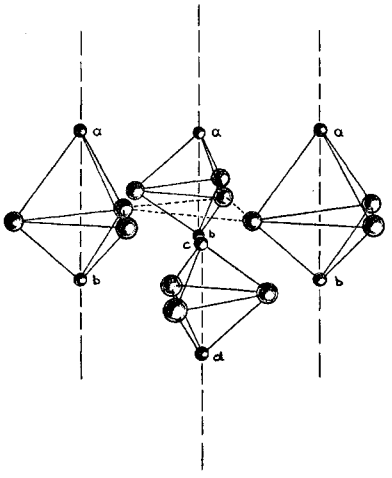

FIG. 3. An Al_2O_3 type (c, d) bipyramid in the foreground with the three nearest upper (a, b) bipyramids indicated.

TABLE VI. Breakdown of bipyramids and clusters contained within sphere of radius $2A_0$. The cluster location scheme is indicated in Fig. 4.

Cluster location	No. of bipyramids	Bipyramid type
1	1	(c, d)
2	6	(c, d)
3	6	(c, d)
4	6	(c, d)
5	2	(a, b)
6	12	(a, b)
7	6	(c, d)
8	6	(c, d)
9	12	(c, d)
10	6	(c, d)
11	6	(a, b)
12	12	(a, b)
13	6	(a, b)
	87	

TABLE VII. Potential sums for various cluster groupings within sphere of radius $2A_0$.

Group No.	1	2	3	4	5	6	7
No. of cells	7	15	21	27	33	33	57
Clusters included	1, 11	1, 5, 8, 11	1, 2, 5, 8, 11	1, 2, 5, 8, 11, 13	1, 2, 5, 8, 10, 11, 13	1, 2, 5, 6, 8, 11	1, 2, 5, 6, 8, 10, 11, 12, 13
1.	17.37495	13.52550	15.89412	16.96679	17.00005	14.68096	16.98304
2.	1.09471	1.42547	0.14567	0.13463	0.40214	0.33417	0.48755
3.	−0.30545	−0.08013	−0.17412	−0.20175	−0.15950	−0.12450	−0.13226
4.	−0.48611	−0.37036	−0.28612	−0.30079	−0.30786	−0.27559	−0.29908
5.	−0.67134	−0.66822	−0.74697	−0.77036	−0.76611	−0.74611	−0.76188
6.	0.22458	0.01515	0.01515	0.04403	0.04923	0.01515	0.04279
7.	−0.14633	−0.14225	−0.14351	−0.14321	−0.14373	−0.14305	−0.14318
8.	−4.31913	−4.30456	−4.23544	−4.24062	−4.23655	−4.23460	−4.23550
9.	−0.48072	−0.70180	−0.70180	−0.68838	−0.68877	−0.70180	−0.69159

that we were able to find, 25.0312, was computed by Schmaeling[10] in 1928 using a simplified crystal geometry and variational methods. From a sphere of radius $6A_0$ containing 2247 cells we find, in conventional units, $M=13.12\times r_{\text{char}}$ (Å). If we take r_{char} as the mean of the Al—O distances (to the upper and lower triangles in Fig. 2), we find $M=25.09$. On the other hand, if r_{char} is the inverse of the mean of the inverse Al—O intervals, $M=25.07$. In view of the precision of the crystallographic special position parameters of Al and O and the degree of convergence of the lattice sum, we do not feel that extension of M beyond four significant figures is warranted.

The next approximation of our potential theory corresponds to the consideration of the lattice as an assembly of point dipoles as well as monopoles. This involves the assigning of polarizabilities as well as the computation of internal electric field components. At the Al sites the only nonzero field component is, of course, E_z, corresponding to $-B_1^0$. The oxygen site symmetry is much lower than that at the aluminum site. It is reasonably evident from geometry that the electric fields at the O sites lie in the basal plane and are directed along the bisectrices of the (small) oxygen triangle angles. This has been borne out by computations similar to those performed previously but now referenced to the O sites. Two new lattice potential terms have to be specified, of course; these are $B_1^1=-E_x=e\sin\theta\cos\varphi/R^2$, $C_1^1=-E_y=e\sin\theta\sin\varphi/R^2$. (Difficulty in computing these electric field strengths led to uncertainty in the earlier work of Brun and Hafner[11] and McClure.) Thus now each bipyramid is an assembly of monopoles and dipoles with zero net dipole moment as well as zero net charge. See Fig. 5. The appropriate lattice potential expression forms[7,12] are listed separately for the oxygen and aluminum dipoles in Tables VIII and IX. The lattice potential terms computed

TABLE VIII. Potential constants for dipolar lattice. Dipoles directed normal to hexagonal axis. $\delta\equiv\varphi-\alpha$, where α is the direction of the dipole vector in the $x-y$ plane.

1. $B_0^0=-(p/R^2)\sin\theta\cos\delta$
2. $B_1^0=-(3p/R^3)\cos\theta\sin\theta\cos\delta$
3. $B_2^0=-(3p/4R^4)\sin\theta(5\cos^2\theta-1)\cos\delta$
4. $B_3^0=-(5p/4R^5)\sin\theta(7\cos^3\theta-3\cos\theta)\cos\delta$
5. $B_3^3=-(5p/8R^5)[7\sin^4\theta\cos3\varphi\cos\delta-3\sin^2\theta\cos(3\varphi-\delta)]$
6. $C_3^3=-(5p/8R^5)[7\sin^4\theta\sin3\varphi\cos\delta-3\sin^2\theta\sin(3\varphi-\delta)]$
7. $B_4^0=-(15p/64R^6)\sin\theta(21\cos^4\theta-14\cos^2\theta+1)\cos\delta$
8. $B_4^3=-(105p/8R^6)\cos\theta[3\sin^4\theta\cos3\varphi\cos\delta-\sin^2\theta\cos(3\varphi-\delta)]$

also

$B_1^1=-(p/R^3)\cdot(3\sin^2\theta\cos\varphi\cos\delta-\cos\alpha)$

$C_1^1=-(p/R^3)\cdot(3\sin^2\theta\sin\varphi\cos\delta-\sin\alpha)$

TABLE IX. Potential constants for dipolar lattice. Dipoles directed along hexagonal axis.

1. $B_0^0=-(p/R^2)\cos\theta$
2. $B_1^0=-(p/R^3)(3\cos^2\theta-1)$
3. $B_2^0=-(3p/4R^4)(5\cos^3\theta-3\cos\theta)$
4. $B_3^0=-(p/4R^5)(35\cos^4\theta-30\cos^2\theta+3)$
5. $B_3^3=-(35p/8R^5)\sin^3\theta\cos3\varphi$
6. $C_3^3=-(35p/8R^5)\sin^3\theta\sin3\varphi$
7. $B_4^0=-(5p/64R^6)(63\cos^5\theta-70\cos^3\theta+15\cos\theta)$
8. $B_4^3=-(3p/8R^6)\sin^3\theta(9\cos^2\theta-1)\cos3\varphi$

also

$B_1^1=-(3p/R^3)\cos\theta\sin\theta\cos\varphi$

$C_1^1=-(3p/R^3)\cos\theta\sin\theta\sin\varphi$

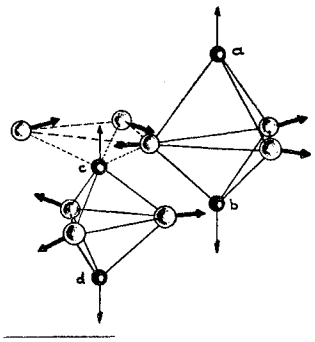

FIG. 5. Bipyramids carrying point dipoles as well as point monopoles.

[10] V. Schmaeling, Z. Physik **47**, 723 (1928), quoted by J. Sherman, Chem. Rev. **11**, 93 (1932).

[11] E. Brun and S. Hafner, Z. Krist. **117**, 63 (1962).

[12] J. Kanamori, T. Moriya, K. Motizuki, and T. Nagamiya, J. Phys. Soc. Japan **10**, 93 (1955).

from these dipolar arrays, of course, are geometrically consistent with the terms from the monopolar array. The actual dipole strengths are then computed in a self-consistent manner after specification of the polarizabilities.

APPLICATIONS TO THE QUADRUPOLE RESONANCE OF Al IN CORUNDUM

The Al^{27} quadrupole resonance in corundum was found first by Pound.[13] Electric field effects have recently been investigated by Bloembergen and Dixon.[14] Pressure experiments have been performed by Veigele.[15] Quadrupole resonance evaluates the product eqQ in which q is the field gradient, $\partial^2V/\partial Z^2$, at the nucleus and Q is the nuclear quadrupole moment. Q had been measured by Lew and Wessel[16] as 0.149×10^{-24} cm^2. To allow for the shielding effects of the electronic clouds q is related to q', the field gradient in the absence of the reference ion, through the Sternheimer antishielding factor γ_∞. The relation is: $q=(1-\gamma_\infty)q'$. In our notation, we identify q' with $4B_2{}^0$. Monopole lattice-sum evaluations of q had been performed by Bersohn[17] and others. Sternheimer factors have been calculated by Das and Bersohn[18] and by Burns.[19] The value of γ_∞ obtained by averaging their results is -2.45. Using the measured eqQ and the independently determined Q value, we then interpret the q evaluation of 2.21×10^{14} cgs units to correspond to a q' of 0.641×10^{14}. Our monopole $B_2{}^0$ value of -0.15149 [eV per unit charge on the O^{2-} ion per Å^3] corresponds to a q' of 0.40424×10^{14} when the appropriate unit conversion factor is used.

The effects of stress upon quadrupole resonance (or electron paramagnetic resonance) have been expressed through a G tensor. However, we will avoid the specific use of such a notation here. If we neglect the effects of lattice vibrations, the changes in q will relate to changes in the lattice sums. If we further assume that the special crystal position parameters w and v are unchanged, the formulas are particularly simple for pressure along the c axis, normal to the c axis, and for hydrostatic pressure. The derivative of $B_2{}^0$ is required: $\partial B_2{}^0/\partial Z=-3B_3{}^0$. Hence $\delta B_2{}^0=-3B_3{}^0\delta Z$. The strain parameter along the c axis, ϵ, by definition is $\delta c/c$ or equivalently $\delta Z/Z$, $(Z\equiv R\cos\theta)$. Hence $\delta B_2{}^0=-3\epsilon(B_3{}^0Z)$; we denote $B_3{}^0Z$ by the symbol $B_3{}^{0*}$. The corundum compliance tensor S_{ij} has been discussed and measured by Wachtman *et al.*[20] We then find the following relations:

Axial pressure $-P$ along the c axis:

$$\frac{1}{P}\frac{\delta q}{q}=3S_{33}\left[\frac{S_{13}}{S_{33}}+\frac{(1-S_{13}/S_{33})B_3{}^{0*}}{B_2{}^0}\right]. \tag{1a}$$

Hydrostatic pressure $-P$:

$$\frac{1}{P}\frac{\delta q}{q}=3\left[S_{11}+S_{12}+S_{13}+\frac{(S_{13}+S_{33}-S_{11}-S_{12})B_3{}^{0*}}{B_2{}^0}\right]. \tag{1b}$$

Pressure $-P$ in basal plane at $\phi=45°$:

$$\frac{1}{P}\frac{\delta q}{q}=\frac{3}{\sqrt{2}}\left\{S_{11}+S_{12}+\frac{[2S_{13}/(S_{11}-S_{12})]B_3{}^{0*}}{B_2{}^0}\right\}. \tag{1c}$$

The $B_2{}^0$ and $B_3{}^{0*}$ expressions in the above equations, of course, represent summations over the entire lattice.

S_{11}, S_{12}, S_{13}, and S_{33} are, respectively, 2.353, -0.716, -0.364, and 2.170×10^{-13} cm^2/dyn. $B_3{}^{0*}=-1.26358$. On this basis we then find $(1/P)\delta q/q$ in (1a), (1b), and (1c) above to be 6.24, 0.806, and -4.38×10^{-12} cm^2/dyn, respectively.

Veigele[15] and his associates in their study of such pressure effects found the c-axis effect to be $2.8\pm0.2\times10^{-12}$ cm^2/dyn. The pressures used ($\sim10^{10}$ dyn/cm^2) were insufficient to detect the hydrostatic effect. A basal plane parameter of -2.7 ± 0.2 was measured but unfortunately the crystal orientation was not known.

We then might inquire how our analyses would be affected by the introduction of point dipoles. Brun and Hafner[11] attempted to evaluate the effect of dipoles on the q' computation. They suggested that the dipolar contribution is opposite in sign to the monopolar contribution and sufficiently large to make q' negative. A negative q' would contradict experiment. However, their analysis is suspect on several points, primarily because they were unable to properly calculate the electric fields at the Al and O sites. As indicated earlier, our use of the Madelung method of summation eliminates these difficulties.

To self-consistently evaluate the Al and O dipoles, the following equations must be solved:

$$\begin{aligned} p_{\mathrm{Al}}&=\alpha_{\mathrm{Al}}[E(\mathrm{Al\ site})+K_1p_{\mathrm{Al}}+K_2p_{\mathrm{O}}],\\ p_{\mathrm{O}}&=\alpha_{\mathrm{O}}[E(\mathrm{O\ site})+K_3p_{\mathrm{Al}}+K_4p_{\mathrm{O}}], \end{aligned}$$

or

$$\begin{aligned} p_{\mathrm{Al}}(1-\alpha_{\mathrm{Al}}K_1)-p_{\mathrm{O}}(\alpha_{\mathrm{Al}}K_2)&=\alpha_{\mathrm{Al}}E(\mathrm{Al\ site}),\\ -p_{\mathrm{Al}}(\alpha_{\mathrm{O}}K_3)+p_{\mathrm{O}}(1-\alpha_{\mathrm{O}}K_4)&=\alpha_{\mathrm{O}}E(\mathrm{O\ site}). \end{aligned} \tag{2}$$

In Eq. (2) the E's denote the monopole contribution to the electric field, the p's the dipole moments, the α's the polarizabilities, and the K's the appropriate factors necessary to specify the dipolar contributions to the electric field. p_{Al} and $E(\mathrm{Al})$ are collinear with c, of course. p_{O} and $E(\mathrm{O})$ are directed along the bisectors of the angles formed by the oxygen triads. To conform to

[13] R. V. Pound, Phys. Rev. **79**, 689 (1950).
[14] N. Bloembergen and R. W. Dixon, Bull. Am. Phys. Soc. **8**, 350 (1963).
[15] W. J. Veigele and J. D. Stettler, Bull. Am. Phys. Soc. **8**, 529 (1963); W. J. Veigele (private communication).
[16] H. Lew and G. Wessel, Phys. Rev. **90**, 1 (1953).
[17] R. Bersohn, J. Chem. Phys. **29**, 326 (1958).
[18] T. P. Das and R. Bersohn, Phys. Rev. **102**, 733 (1956).
[19] G. Burns, J. Chem. Phys. **31**, 1253 (1959).
[20] J. B. Wachtman, W. E. Tefft, D. G. Lam, and R. P. Stinchfield, J. Res. Natl. Bur. Stds. **64A**, 213 (1960).

McClure's notation we express E in electron volts per unit charge on the O^{2-} ion per Å^2, p in electron volts—Å per unit charge on the O^{2-} ion, α in Å^3 and K in Å^{-3}. We also have

$$B_2^0 = -0.15149 - 0.02229 p_{Al} - 0.12168 p_O$$

or equivalently in the usual cgs units (using the conversion factor -2.6684×10^{14}):

$$q'\times10^{-14} = 0.40424 + 0.05948 p_{Al} + 0.32469 p_O. \quad (3)$$

From our computations over a radius of $4A_0$, we find $K_1=0.10012$, $K_2=-0.80877$, $K_3=-0.53913$, $K_4=-0.04313$, $E(\mathrm{Al})=-0.40966$, and $E(\mathrm{O})=-0.38601$. From a simplified analysis of appropriate corundum data Tessman *et al.*[21] had evaluated α(Al) as 0.05 and α(O) as 1.34. Such oversimplified procedures in evaluating polarizabilities have been criticized recently by Bolton *et al.*[22] However, in the particular case of corundum, as discussed later, the Tessman method is quite appropriate. We therefore will consider the Tessman data to provide a reasonable estimation for the α's. We find $p_{Al}\simeq-0.010$, $p_O=-0.488$; hence $q'=0.240\times10^{14}$. Whereas the monopolar calculation had yielded a q' which was 63% of the expected value, the inclusion of dipolar effects has reduced q' to 37%. The dipolar contributions to the pressure formulas Eqs. (1a)–(1c) will occur primarily in the denominators through modification of B_2^0 since dipolar contributions to B_3^{0*} are not very significant. We now find (1a), (1b), (1c) to be 10.34, 1.08, -7.43×10^{-12}, respectively.

The numerical results seem to be sufficient to indicate that the Brun and Hafner[11] suggestion (that the dipolar contribution would predominate over the monopolar contribution and make q' negative) is inadmissible. Whether one can infer from these calculations and existing resonance and pressure data a measure of the covalency of the Al—O bonds is a difficult point. (We have also computed the change in q associated with changes in the special position parameters w and v. We find $(\delta q/q)=3.7\delta w/w$, $\delta q/q=16.7\delta v/v$. Unfortunately, pressure-dependent variations of v and w sufficient to contribute significantly to Veigele's results would still be undetectable by x-radiation analysis.) Laurance *et al.*[23] had concluded from their studies of Al hyperfine interactions in ruby that the covalent bonding is of the order of 20%. They suggest that such effects could produce the needed increment in q'. We believe that the stress-induced changes expected from this "covalent" q' contribution are small. Multiplying our final results by 0.37 to allow for the increase in the denominator then yields (1a), (1b), (1c) values of 3.8, 0.4, -2.8×10^{-12}, respectively. The available data[15] for (1a) and (1c), 2.8 and -2.7×10^{-12}, are in reasonable agreement. The (1b) value was insufficient for detection.

TABLE X. Electric effect R tensor in C_3 symmetry. There are five independent constants: R_{111}, R_{222}, R_{333}, R_{123}, and R_{113}. In C_{3v} symmetry $R_{111}\equiv0$, $R_{123}\equiv0$ and three independent constants remain.[a]

R_{111}	$-R_{111}$	0	R_{123}	R_{113}	$-2R_{222}$
$-R_{222}$	R_{222}	0	R_{113}	$-R_{123}$	$-2R_{111}$
R_{311}	R_{311}	R_{333}	0	0	0

$$R_{311}=-\tfrac{1}{2}R_{333}$$

[a] $\mathcal{H}_E=\sum_{ijk\,j\leq k}\tfrac{1}{2}R_{ijk}E_i(S_jS_k+S_kS_j)$.

RUBY. Cr^{3+} IN CORUNDUM

The gem "ruby" is obtained when a small number of the Al^{3+} ions in corundum are replaced substitutionally by Cr^{3+} ions. Experimentally it has been found that the nature of the symmetry about an occupied site does not change from that in corundum. The simplest explanation is that substitution occurs without any modification in atom positions although more general distortions conforming to the C_3 point symmetry can easily be envisaged.

The gross features of the optical spectra are related to the cubic field parameter $10Dq$ and to the trigonal field parameter v. (The trigonal field "v" is not to be confused with the crystallographic parameter "v.") To be consistent with our coordinate system and geometry these are defined as follows:

$$10Dq=-\left[\frac{3\sqrt{2}}{4}B_4^3+\frac{4}{27}\left(B_4^0+\frac{B_4^3}{20\sqrt{2}}\right)\right]\frac{4}{21}\langle r^4\rangle,$$
$$v=-\frac{6}{7}B_2^0\langle r^2\rangle+\frac{160}{63}\left(B_4^0-\frac{B_4^3}{20\sqrt{2}}\right)\langle r^4\rangle. \quad (4)$$

$\langle r^2\rangle$ and $\langle r^4\rangle$ represent the appropriate averages over the radial portion of the d-electron wave function. Another spectral parameter of interest is what we will call τ, the enhancement of the measured eqQ for the Al nearest (either above or below) the Cr. [For example, if position (c) in a bipyramid is occupied by a Cr ion, the eqQ of the Al in position (d) is equal to the value in bulk corundum multiplied by τ.] Although the theoretical evaluation of eqQ is a subtle problem, we anticipate that relative changes are readily calculable. A fourth parameter is the "skew angle" β determined from the electric effect R tensor. The R tensor (Table X) relates the electron paramagnetic resonance Hamiltonian to applied electric field. In C_3 symmetry there are five independent constants[24]: R_{111}, R_{222}, R_{333}, R_{123}, and R_{113}

[21] J. R. Tessman, A. H. Kahn, and W. Shockley, Phys. Rev. **92**, 890 (1953).

[22] H. C. Bolton, W. Fawcett, and I. D. C. Gurney, Proc. Phys. Soc. (London) **80**, 199 (1962).

[23] N. Laurance, E. C. McIrvine, and J. Lambe, Phys. Chem. Solids **23**, 515 (1962).

[24] E. B. Royce and N. Bloembergen, Phys. Rev. **131**, 1912 (1962).

(in C_{3v} symmetry R_{111} and R_{123} must vanish identically). R_{113}, R_{222}, and R_{333} relate to B_1^0, B_3^0, and B_3^3 while R_{123} and R_{111} relate to C_3^3. The R components for the four possible Cr sites then transform as the appropriate B's and C's do in Table III. If we fix our attention upon a particular Cr type of site such as (c), we can rotate our coordinate system about the c axis and transform the R_{ijk} values *for that site* so as to make R_{123} and R_{111} zero in the *new* coordinate system. The rotation required defines our skew angle β. Since in this new coordinate system the C_3^3 value, $(C_3^3)'$, is necessarily zero it follows from geometry that β is related to the C_3^3 and B_3^3 values in the *standard* coordinate system as follows:

$$\beta=\tfrac{1}{3}\tan^{-1}(C_3^3/B_3^3). \tag{5}$$

Numerically $10Dq$ is about 18 150 cm^{-1}; v ranges from 1050 to 1425 cm^{-1},[7] depending upon the detailed interpretation of the spectra, τ is 1.47 (Ref. 23), and $|\beta|$ is $5.5\pm1.0°$.[24] To evaluate v and $10Dq$, values for $\langle r^2\rangle$ and $\langle r^4\rangle$ are needed to supplement the lattice sum compilations. We selected the tables of Ballhausen and Ancmon[25] for this purpose. These authors tabulate various radial integrals evaluated from hydrogen-type wave functions. Inner and outer forms of the solutions are matched at a ligand distance r_0. We chose 5 as the effective nuclear charge seen by a $3d$ electron of Cr^{3+} and set $r_0=1.9125$ Å from crystal geometry. We find $\langle r^2\rangle=1.32$ Å^2, $\langle r^4\rangle=2.47$ Å^4. We will "adjust" the $\langle r^4\rangle$ value to fit the experimental $10Dq$ and scale $\langle r^2\rangle$ similarly, keeping $\langle r^4\rangle/\langle r^2\rangle$ fixed.

The simple substitution of Al for Cr without change in lattice geometry then yields from Table V and Eqs. (4) and (5) the "adjusted" $\langle r^n\rangle$ values $\langle r^4\rangle=1.31$ Å^4, $\langle r^2\rangle=0.70$ Å^2, and $v=-1115$ cm^{-1}, $\tau=1.0$, and $\beta=-1.1°$. Clearly this is an unsatisfactory solution. McClure had in a similar manner computed a negative v value. (His paper was prepared before the experimental τ and β results were available.) McClure was then able to fit $10Dq$ and v by translating the Cr ion about 0.1 Å along the c axis away from the Al below—but this still leads to unsatisfactory results for τ and β: $\tau=0.60$, $\beta=0.7°$. The Cr ion in McClure's model is displaced to a relatively eccentric position with Cr—O nearest-neighbor distances equal to 2.03751 and 1.81312, averaging to 1.92532 as compared to the Al—O values of 1.96886 and 1.85619 averaging to 1.91253. The corresponding distances in Cr_2O_3 are 2.01551 and 1.96512 averaging to 1.99032 (all in Å).

Artman and Murphy[26] have suggested that a more realistic model should permit distortion of the Cr environment in a more general fashion still consistent with C_3 point symmetry. Since Cr^{3+} is ~0.1 Å larger than Al^{3+} by most chemical criteria (for instance, note the cation-anion intervals for Al_2O_3 and Cr_2O_3 cited in the previous paragraph) a model was postulated in which the Cr nearest-neighbor oxygen triangles could expand as well as move vertically along the c axis. The upper triangle twist α was not varied since the crystallographic parameter v (and hence α) has the same value in both pure Al_2O_3 and pure Cr_2O_3; see Table I. The Cr ion and the Al below it were permitted to shift along the c axis. See Fig. 6.

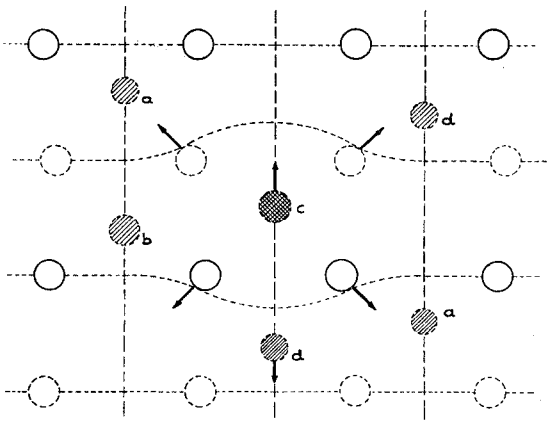

FIG. 6. Distortion of the corundum lattice by a Cr ion entering as an Al substituent on a type (c) site.

Initially, the lattice sums for a monopolar lattice were used. For each proposed model, the $10Dq$ value was matched as explained previously and then the results for v, τ, and β were computed. In order to get a reasonable fit to the data it was necessary to expand the local environment primarily upward and outward toward the "empty" site. The resultant local geometry is shown in Fig. 7 together with the corresponding dimensions in Al_2O_3 and Cr_2O_3. In this ruby model the upper oxygen triangle was pushed upward 0.115 Å while its "radius" was increased from 1.655 to 1.751 Å. The lower oxygen triangle was pushed downward 0.02 Å. The Cr was moved upwards 0.03 Å while the Al was moved downwards 0.02 Å. The mean Cr—O distance for this model corresponded to 1.99185 Å, very close to the Cr_2O_3 value of 1.99032. After matching $10Dq$, $\langle r^4\rangle$ was set equal to 1.68 Å^4, $\langle r^2\rangle$ to 0.87 Å^2, 65% of the values originally selected from the Ballhausen-Ancmon tables. The trigonal field parameter v was found to equal 671 cm^{-1}, τ to 1.35, and β to $-4.9°$. [The empirical closeness of β to the geometrical skew angle α (3.9°) is in our view a fortuitous result.]

Our fit to the trigonal field parameter v differs in an important aspect from that of McClure. If the unmodified corundum lattice geometry is used, the computed v is negative since a negative contribution from the B_2^0 term is larger than a positive contribution from the $B_4^0-B_4^3$ term. By shifting the Cr upward 0.1 Å, McClure obtained a positive v value since now the negative B_2^0 contribution was overridden by a positive

[25] C. J. Ballhausen and E. M. Ancmon, Kgl. Danske Videnskab. Selskab, Mat. Fys. Medd. **31**, No. 9 (1958).

[26] J. O. Artman and John C. Murphy, Bull. Am. Phys. Soc. **8**, 323 (1963).

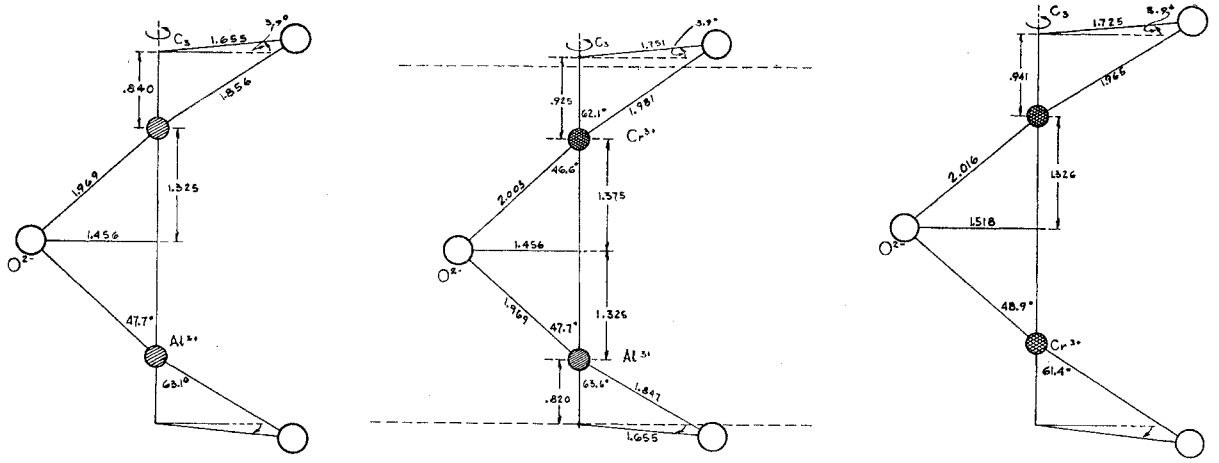

(a) (b) (c)

FIG. 7. Local geometry about: (a) an Al site in corundum, (b) a Cr site in ruby, (c) a Cr site in Cr_2O_3.

$B_4^0-B_4^3$ term. In our case, however, a *positive* B_2^0 term is partially compensated by a *negative* $B_4^0-B_4^3$ contribution. These distinctions are important when considering the quadrupole splittings of various ions substituted for Al in corundum. It has generally been presumed that the field gradient $4B_2^0$ is *positive* in conventional units (this it will be recalled corresponds to a negative B_2^0 in the units used in this paper) for these substituents as it is for Al. See, for example, Terhune *et al.*[27] Our analysis would suggest that the field gradient for Cr^{3+} in corundum is *negative*. We will return to this matter later.

The next logical step in our ruby model computations is the introduction of dipolar lattice sums. We had shown earlier that the contribution of the aluminum dipoles is small; hence only the oxygen dipoles were considered. Accordingly, the monopolar lattice fields at the upper and lower nearest-neighbor oxygens were evaluated. As a consequence of the distortion, z-directed dipoles were induced in the oxygen ions with dipole moment values of 0.29 and 0.46 for upper and lower oxygens, respectively. The value of α_O used was, as before, 1.34 Å^3. (It will be shown later that $\alpha_{O\parallel}\simeq\alpha_{O\perp}$.) In addition, the basal plane dipoles were modified both in magnitude and direction from those of corundum. The upper oxygen dipoles were each rotated back by 41° and decreased to −0.41; the lower oxygens were rotated back by 10° and increased to −0.59 in value. The oxygens in the remainder of the lattice were assigned the standard corundum oxygen dipole orientations and the previously evaluated dipole moment value of −0.50. [The contributions of the oxygen dipole array to the electric fields at these displaced nearest-neighbor oxygen were also computed. These were found to be relatively small when compared to the monopolar lattice contribution. Within the spirit of this calculation they have been omitted for simplicity. Note, for example, the numerical solutions of Eq. (2) earlier in the paper.] If the same geometry and $\langle r^2\rangle$, $\langle r^4\rangle$ values as before are maintained, we find a $10Dq$ of 18 307 cm^{-1}, v of 1246 cm^{-1}, τ of 1.40 and β of −6.9°. Hence the

TABLE XI. Monopolar and dipolar potential constants for a type (*c*) Cr site in corundum. The local geometry corresponds to Fig. 7(b) of this paper.

	Monopolar sums		Oxygen dipolar sums	
	nn $\bar{R}=1.99185$	$R=4A_0$ 683 cells	*nn*	$R=4A_0$
1. B_0^0	43.37511	15.67016	0.17748	0.35496
2. B_1^0	−2.24874	−0.05848	−0.54633	−0.49980
3. B_2^0	0.07708	0.09477	0.08397	0.07546
4. B_3^0	−0.32926	−0.18588	0.06900	0.06389
5. B_3^3	−0.54210	−0.44583	0.07056	0.07993
6. C_3^3	−0.24603	0.11787	0.02691	0.02014
7. B_4^0	−0.11210	−0.12388	−0.00588	−0.00581
8. B_4^3	−3.50717	−3.31008	−0.02541	−0.02798

TABLE XII. Comparison between experimental and computed ruby spectral data. The geometry of Fig. 7(b) was used.

	Experimental values	Values computed from theory using the model presented in this paper: Monopolar lattice	Monopolar and oxygen dipolar lattice
$10Dq$	18 150 cm^{-1}	matched to experimental datum	18 307 cm^{-1}
v	1050–1425 cm^{-1}	671 cm^{-1}	1246 cm^{-1}
β	$\lvert\beta\rvert=5.5\pm1.0°$	−4.9°	−6.9°
τ	1.47	1.35	1.40
$\langle r^2\rangle$		0.87 Å^2	
$\langle r^4\rangle$		1.68 Å^4	

[27] R. W. Terhune, J. Lambe, C. Kikuchi, and J. Baker, Phys. Rev. **123**, 1265 (1961).

addition of dipolar contributions does not vitiate the results derived previously from the monopolar model—in fact, the correspondence with experiment is, in general, improved. The data are presented in Tables XI and XII.

OPTICAL INTENSITY FORMULAS AND THE OPTICAL ELECTRIC EFFECT

Sugano and Tanabe[28] had presented formulas for the ruby $U[^4T_2(t_2^2e) \rightarrow {}^4A_2(t_2^3)]$ and $Y[^4T_1(t_2^2e) \rightarrow {}^4A_2(t_2^3)]$ band intensities which were valid only under very restrictive conditions. Taking into consideration the complete set of odd crystal field elements, McClure subsequently derived more general formulas for Cr^{3+} as well as other transition metal ions in corundum. Independently we also had derived such formulas for Cr^{3+} in corundum[29] and had discussed them previously using the lattice sums of McClure's $+0.1$ Å displacement model. In view of the ruby distortion model presented in this paper, we would like to bring our discussion up to date, quoting just the end results and referring those interested in details to Ref. 29.

The dipole strength formulas are

$$|P|_{U_\parallel}{}^2=(1/108)(2C_PS_1+C_2S_2)^2(\bar{V}_P\bar{V}_{X2})^2\cdot\Delta^{-2},$$

$$|P|_{U_\perp}{}^2=(1/4)|P|_{U_\parallel}{}^2+(1/36)(CS_2-C_P)^2\times(\bar{V}_P\bar{V}_{X1})^2\cdot\Delta^{-2},$$

$$|P|_{Y_\parallel}{}^2=(1/81)\{(CS_3+C_P)\bar{V}_P\bar{V}_{X1}+6^{1/2}C_PS_4\bar{V}_P\bar{V}_{XA}\}^2\cdot\Delta^{-2},$$

$$|P|_{Y_\perp}{}^2=(1/324)\{(CS_3+C_P)\bar{V}_P\bar{V}_{X1}+2(6)^{1/2}C_PS_4\bar{V}_P\bar{V}_{XA}\}^2\cdot\Delta^{-2}+(1/432)(3C_2S_3+2C_PS_1)^2(\bar{V}_P\bar{V}_{X2})^2\cdot\Delta^{-2},$$

where

$$\bar{V}_{X1}=(\bar{V}_{X1})_a+(\bar{V}_{X1})_b,$$

$$C\bar{V}_{X1}\equiv C_1(\bar{V}_{X1})_a-\tfrac{3}{2}C_2(\bar{V}_{X1})_b,$$

$$\Delta=W(^4T_{2u})-W(^4A_{2g}),$$

$$S_1=\Delta/[W(^4T_{1u})-W(^4A_{2g})],$$

$$S_2=\Delta/[W(^4T_{2u})-W(^4T_{2g})],$$

$$S_3=\Delta/[W(^4T_{2u})-W(^4T_{1g})],$$

and

$$S_4=\Delta/[W(^4A_{1u})-W(^4A_{2g})].$$

The intensity formulas above have an additional factor of 3 in the numerator over those of Ref. 29. This reflects a multiplication of the reduced matrix elements involving A_2 by $\sqrt{3}$ (Table 4, Ref. 29) which is necessary when the wave functions are properly antisymmetrized.[30] The necessary one-electron reduced matrix element relations are listed in Table XIII. (These involve corrections from the listing in Table 5, Ref. 29.) It will be noted that the t_1-t_2 and t_1-e matrix element ratios for

TABLE XIII. Various relations involving reduced matrix elements. The group representations are taken from S. R. Polo, "Fundamentals of Crystal Field Theory, Vol. II. Tables" (RCA Laboratories, unpublished). The usage of B_1^0, B_3^0, B_3^3 and C_3^3 follows that of D. S. McClure, Ref. 7. The radial integrals I_n are given by $\int R_{4p}r^nR_{3d}dr$.

V_{X1}—representations of $(T_{10})_u$

$(V_{X1})_a \propto r^1Y_1^0 \quad (V_{X1})_b \propto \frac{1}{3}r^3[2Y_3^0-(5/2)^{1/2}(Y_3^3-Y_3^{-3})]$

$t_1\|(V_{X1})_{a,b}\|t_2=(\bar{V}_{X1})_{a,b}$

$(\bar{V}_{X1})_a=(6/5)^{1/2}B_1^0I_1 \quad (\bar{V}_{X1})_b=(4/7)(3/5)^{1/2}(\sqrt{2}B_3^0+B_3^3)I_3$

$t_1\|(V_{X1})_a\|e=C_1(2/3)^{1/2}t_1\|(V_{X1})_a\|t_2$

$t_1\|(V_{X1})_b\|e=-C_2(3/2)^{1/2}t_1\|(V_{X1})_b\|t_2$

V_{XA}—representation of $(A_2)_u$

$V_{XA}\propto\frac{1}{3}r^3[5^{1/2}Y_3^0+\sqrt{2}(Y_3^3-Y_3^{-3})]$

$t_1\|V_{XA}\|t_2=\bar{V}_{XA} \quad \bar{V}_{XA}=-(2/7)(1/10)^{1/2}(5\sqrt{2}B_3^0-4B_3^3)I_3$

V_{X2}—representation of $(T_{20})_u$

$V_{X2}\propto(r^3/\sqrt{2})(Y_3^3+Y_3^{-3})$

$t_1\|V_{X2}\|t_2=\bar{V}_{X2} \quad \bar{V}_{X2}=-[12/7(5)^{1/2}]C_3^3I_3$

$t_1\|V_{X2}\|e=(C_2/\sqrt{2})t_1\|V_{X2}\|t_2$

V_P is of the same form as $(V_{X1})_a$. Hence $C_P=C_1$.

V_{X1a} and V_{X1b}, respectively, the r^1 and r^3 contributions to the $(T_{10})_u$ crystal field representation, are different both in magnitude and sign. Unfortunately, this is not at all evident from the paper of Sugano and Tanabe.[28] [A similar effect involving the t_2-t_2 and t_2-e matrix element ratios for the r^2 and r^4 components of the $(T_{20})_g$ trigonal crystal field is evident from Eqs. (5) and (6) of McClure. The corresponding Sugano and Tanabe analysis applies only to the r^2 component.] Because of differences in notation it may be difficult to ascertain any difference between our formulas and those of McClure. McClure purposely simplified his derivations by setting the quantities which correspond to our C_i and S_i equal to unity. Partially because of the difficulty in computing B_1^0 convergently, McClure also introduced a parameter $x=B_1^0\langle r\rangle/\langle r^3\rangle$ which was variously set plus or minus to fit the different transition metal optical data. In our case, given a model, there is no uncertainty in B_1^0, computationally speaking. We note further that due essentially to the off-diagonal nature of the radiation matrix elements, combinations of V_P (type T_{1u}) with V_{X2} [type $(T_{20})_u$] as well as V_{X1} [type $(T_{10})_u$] are permitted. The experimental optical data from McClure yield $|P|_{U_\parallel}{}^2=1.49$, $|P|_{U_\perp}{}^2=5.67$, $|P|_{Y_\parallel}{}^2=9.41$ and $|P|_{Y_\perp}{}^2=5.12$ all in (debye)^2 or $(10^{-18}$ esu·cm$)^2$.

To compare our dipole strength formulas to these data will require information on matrix elements such as $\bar{V}_P\bar{V}_{X1}/\Delta$. Since the optical electric-effect results assist in this evaluation, we will digress to the electric effect and then return to the matrix element evaluation at the close of this section.

Optical Electric Effect

By the electric effect (EE) we will refer to the shift in energy levels upon application of an electric field. Such

[28] S. Sugano and Y. Tanabe, J. Phys. Soc. Japan 13, 880 (1958).

[29] J. O. Artman and John C. Murphy, *Proceedings of the First International Conference on Paramagnetic Resonance*, edited by W. Low (Academic Press Inc., New York, 1963), p. 634.

[30] M. G. Cohen (private communication).

shifts are proportional to odd symmetry matrix elements.

$$\begin{aligned}\mathrm{EE} \propto \tfrac{1}{2}[V(\text{odd crystal})+V(\text{odd applied})]^2 \\ -\tfrac{1}{2}[V(\text{odd crystal})]^2 \\ = V(\text{odd crystal})V(\text{odd applied}) \\ +\tfrac{1}{2}[V(\text{odd applied})]^2.\end{aligned}$$

The first term corresponds to the linear Stark effect, the second to the quadratic Stark effect. The optical electric effect in ruby (ROEE) will refer to the removing of the geometrical degeneracy of the R lines by an applied electric field. For a type (c) site the shift of the R line by an electric field in the Z direction is

$$\begin{aligned}\mathrm{ROEE} &= \mathrm{OEE}(^2E_g)-\mathrm{OEE}(^4A_{2g}) \\ &= \tfrac{2}{3}\bar{V}_{X1}\bar{V}_A\Delta^{-1}\left[1-\frac{\frac{1}{4}\Delta}{W(^2T_{1u})-W(^2E_g)}\right. \\ &\qquad \left.-\frac{\frac{1}{3}\Delta}{W(^2T_{2u})-W(^2E_g)}\right]. \qquad (6)\end{aligned}$$

[Equation (6) differs from the corresponding relation in Refs. 29 and 31 by a correction of 3 due to proper antisymmetrization and additional corrections to the ^2E_g contribution.] The $\bar{V}_A$ and previously defined $\bar{V}_P$ matrix elements are identical save for the value of the *effective* electric field at the Cr site, $\bar{V}_A=\bar{V}_P E_{\mathrm{Cr}}$. Combinations of the form $\bar{V}_{X2}\bar{V}_A$ are not permitted here. It is also clear from symmetry that no first-order shifts are expected for fields applied normal to the c axis.

Polarization Contributions to the Effective Field

The internal effective polarizing field E(local) can be written as the sum of three parts: (1) V/d, the external field; (2) $\frac{4}{3}\pi P$, the self-effect correction using the uniform macroscopic polarization P; (3) $P_L=(L-\frac{4}{3}\pi)P$, the additional self-effect correction. The last is obtained when the local deviation of the polarization from the macroscopic value is approximated by a sum over a point dipole lattice evaluated at the field point of interest. The correlation between microscopic and macroscopic polarization effects in crystals has recently been discussed by Bolton *et al.*[22] and earlier by Tessman *et al.*[21] The former have extended the Clausius-Mossotti (C-M) relation to anisotropic electronic polarizability $\boldsymbol{\alpha}$. Assuming the C-M relation to be valid for optical frequencies, they obtain

$$\frac{(\alpha_m)_j}{V_M}=\frac{\mu_j^2-1}{L_j(\mu_j^2-1)+4\pi}, \quad j=\|,\perp. \qquad (7)$$

We will use this equation and the L_j values which we have obtained from our dipolar lattice calculation.

If we consider our lattice as a collection of bipyramidal Al_2O_3 "molecules," we find the *molecular* $(l-\frac{4}{3}\pi)_{\|}$ and $(l-\frac{4}{3}\pi)_{\perp}$ factors to be 0.00952 and -0.00476, respectively. Upon multiplication by the molecular volume, 43.5 Å^3, these correspond to 0.414 and -0.207, respectively, which yield $L_{\|}=4.603$, $L_{\perp}=3.982$. Since the resultant anisotropy in L far outweighs the anisotropy in μ, Eq. (7) can be made consistent only if $\alpha_{\perp}/\alpha_{\|}=1.07$.

Suppose, on the other hand, we consider the oxygens and aluminums individually. We will assume that to first order the effective local field at each site is the same. We will neglect Al dipoles. We find upon averaging over the five vertices of the bipyramid that $(l-\frac{4}{3}\pi)_{\|}=-0.00622$ and $(l-\frac{4}{3}\pi)_{\perp}=0.00311$. Dividing by 3 (so as to count each oxygen only once) and multiplying by 43.5 we get -0.0901 and 0.0451, respectively, yielding $L_{\|}=4.098$, $L_{\perp}=4.234$. The anisotropy in L derived by this method is in the opposite sense and much less in magnitude than before! Equations (7) are now consistent with $\alpha_{\|}/\alpha_{\perp}=1.006$. We will assume the second model to be the more appropriate. Hence, in the Z direction we can write the field E(local) at one of the constituent ions of the corundum bipyramid as

$$\begin{aligned}(E_{\mathrm{loc}})_i &\simeq E+\tfrac{4}{3}\pi P-0.0901P+P_i, \\ P_i(i=\mathrm{Al}) &= -0.4106P, \\ P_i(i=\mathrm{O}) &= 0.2737P,\end{aligned} \qquad (8)$$

where

$$\begin{aligned}\langle(E_{\mathrm{loc}})_i\rangle_{\mathrm{av}}{}^{(i)} &= E+\tfrac{4}{3}\pi P-0.0901P, \\ P &= (K-1)E/4\pi.\end{aligned}$$

Although our ruby model is one in which the environment is distorted we will assume that Eq. (8) is sufficiently valid at a Cr site for our purposes. We will then use this equation for dc voltages employing the low-frequency value of K. We then have

$$\begin{aligned}E_{\mathrm{Cr}} &= V/d+\tfrac{4}{3}\pi P-0.50P, \\ P &= (K-1)(V/d)/4\pi.\end{aligned}$$

The observed low-frequency dielectric constant $K_{\|}$ is 11.3.[32] Since μ^2 gives 3.1, the low-frequency constant is 27% electronic and 73% ionic. We can regard the $0.50P$ correction to E_{Cr} either as a modification in the crystal field proportional to the applied field or as a geometrical structure sensitive addition to the applied field with the crystal field maintained constant. We further note that operationally speaking, we are unable to distinguish between the electronic and ionic contributions to P as far as "electric effects" are concerned.

Evaluation of Matrix Elements

Thus, we find $E_{\mathrm{Cr}}=4.02(V/d)$. Recent work by Naiman and Linz[33] has suggested that the quartet and

[31] J. O. Artman and John C. Murphy, J. Chem. Phys. **38**, 1544 (1963).

[32] Massachusetts Institute of Technology, Laboratory for Insulation Research, Tech. Repts. 57, 119 and 126 (unpublished).

[33] C. S. Naiman and A. Linz, *Proceedings of the Polytechnic Institute of Brooklyn Conference on Optical Masers* (John Wiley & Sons Inc., New York, 1963), p. 369.

doublet odd-parity states cluster about 57 000 cm^{-1} above the ground level. The { } factor in the ROEE expression[6] then equals 0.218. The R line splitting of 1.0 cm^{-1} observed by Kaiser, Sugano, and Wood[34] at an applied field of 1.7×10^5 V/cm corresponds to an individual site shift of 0.5 cm^{-1}. We then have from ROEE:

$$\bar{V}_{X1}\bar{V}_P/\Delta=0.300 \text{ debye}.$$

Similar matrix elements can be extracted from the optical dipole strengths. The U band formulas are the most convenient to use. After correcting for index of refraction by dividing by $(\mu^2+2)^2/9\mu$, manipulating and taking square roots, these yield:

$$(CS_2-C_p)\bar{V}_{X1}\bar{V}_P/\Delta=1.08 \text{ debye}, \quad (9a)$$

$$(2C_pS_1+C_2S_2)\bar{V}_{X2}\bar{V}_P/\Delta=0.99 \text{ debye}. \quad (9b)$$

Our procedure will be, first, to fit Eq. (9a). As a check upon the internal consistency of the parameters used in this fit, we will then examine Eq. (9b) and the Y band intensity formulas to see if they scale properly.

From the Ballhausen-Ancmon tables we find $I_1=-0.260$ Å, $I_3=-0.817$ Å^3 for $Z_{3d}=5$, $Z_{4p}=3$. We will accept the I_3/I_1 ratio of 3.14 Å^2 as valid. We set $S_2\simeq1.47$ and $C_2\simeq\frac{1}{2}C_1$. We find $C=0.035C_1$ and finally from (9a) $C_1\bar{V}_{X1}\bar{V}_P/\Delta=1.14$. For (9b) we will need in addition S_1 which we approximate as 1.00. Using just the C and S parameters we find $C_1\bar{V}_{X2}\bar{V}_P/\Delta=0.36$; hence, $\bar{V}_{X2}/\bar{V}_{X1}=0.316$. On the other hand, if we compute $\bar{V}_{X2}/\bar{V}_{X1}$ from the entries in Table XI together with our I_3/I_1 value, we find $\bar{V}_{X2}/\bar{V}_{X1}=0.245$. Our $\bar{V}_{X2}/\bar{V}_{X1}$ value inferred from use of the C and S parameters is thus 29% larger than the value "directly" computed. For the Y band formulas we need the additional parameters $S_3\simeq1.77$, $S_4\simeq1.00$. We find with the use of the appropriate C and S values that $|P|_{Y_{II}}$ and $|P|_{Y_I}$ are, respectively, 33% and 18% too high over the values found by "direct" computation from Table XI. In view of the crudeness of the model we do not regard these overages as excessive. (We have not bothered to adjust the constants for a still better fit.) We also note that a match to the $V_{X1}V_P/\Delta$ value of 0.300 derived from ROEE would require $C_1=3.8$.

Returning to the ROEE, Eq. (6), we set $\Delta=57\times10^3$ cm^{-1}, $\bar{V}_{X1}=-1.222I_1-0.478I_3=-2.722I_1$ for $I_3/I_1=3.14$, $\bar{V}_A/E_{Cr}=(6/5)^{1/2}I_1$. Using the conversion factor of 0.8066×10^4 cm^{-1}/eV, we find $|I_1|=0.84$ Å. This represents a multiplication of the Ballhausen-Ancmon table result by 3.3. Nevertheless, the value of $\langle z\rangle_{3d-4p}$ is still quite reasonable, for example. We have $\langle z\rangle=[2/(15)^{1/2}]I_1$; hence $\langle z\rangle=0.43$ Å. Further, we compute $\bar{V}_{X1}=-2.29$ eV or equivalently -18.5×10^3 cm^{-1}, $\bar{V}_{X2}=-0.560$ eV (-4.52×10^3 cm^{-1}), $\bar{V}_{XA}=0.287$ eV (2.32×10^3 cm^{-1}).

[34] W. Kaiser, S. Sugano, and D. L. Wood, Phys. Rev. Letters **6**, 605 (1961).

THE MICROWAVE ELECTRIC EFFECT

Rado,[35] from Cr_2O_3 magnetoelectric effect studies, has suggested that the ruby $^4A_2$ ground-state splitting $2D$ could be affected by application of an electric field. The proposed mechanism involved fourth-order perturbation matrix elements of the form V(odd crystal) V(odd applied)V(spin-orbit)$^2/(\Delta W_1\Delta W_2\Delta W_3)$. Upon application of an electric field along the c axis, the ruby $\frac{3}{2}\leftrightarrow\frac{1}{2}$ and $-\frac{3}{2}\leftrightarrow-\frac{1}{2}$ microwave transitions would split into two inasmuch as the effect for the (a,c) sites would be opposite to that for the (b,d) sites. This ruby microwave electric effect was found first by Artman and Murphy.[36] Bloembergen[24] has shown that the more general tensorial description of this effect consistent with crystal symmetry leads to the decomposition of the single microwave resonance into four (i.e., one for each site type) with appropriately oriented electric and magnetic fields.

In our earlier analyses[29] we pointed out the difficulty of evaluating in detail the many perturbation loops contributing to the matrix element. We suggested that the microwave electric effect (MEE) could be written in the form (we include the correction factor of 3 here):

$$\text{MEE}=\delta_E(2D)=-\tfrac{2}{3}\bar{V}_{X1}\bar{V}_A\Delta^{-1}h_1(V_{so}/\Delta W), \quad (10)$$

where h_1 is a second-degree function of $V_{so}/\Delta W$. Experimentally MEE equals 1.77×10^{-8} cm^{-1} per V/cm.[36] The numerical value of $\bar{V}_{X1}\bar{V}_A\Delta^{-1}$ could be obtained from the ROEE. Our earlier estimation of h_1 as 6×10^{-3}, necessary to fit the experimental results, has been criticized as being excessive. We wish to point out here that the presently revised ROEE and MEE formulas reduce materially the required value of h_1.

Since experimentally MEE/ROEE is 6×10^{-3} we find from (6) and (10) that h_1 equals 1.3×10^{-3}. We also note that our downward revision of Δ from 70 to 57×10^3 cm^{-1} will tend to decrease the magnitude of the spin-orbit contribution required in the numerator of h_1. Very recently Cohen and Bloembergen[37] have reported a ROEE value 29% larger than that of Kaiser *et al.*[34] Acceptance of this new result would reduce h_1 correspondingly, to about one-sixth of our original value.[29]

GROUND-STATE SPLITTING $2D$

Traditionally the mechanism responsible for the splitting of the $^4A_2$ ground state was taken as[28] $|V(\text{spin-orbit})|^2[v/(\Delta W_1\Delta W_2)]$. A correlation between the ^2E state splitting which depends partly on v, $2D$, and the trigonal field separations of the optical bands is expected. However, the Sugano and Peter[2] diagonalization of the energy matrix by machine methods (extending the previous Sugano and Tanabe[28] calculations),

[35] G. T. Rado, Phys. Rev. Letters **6**, 609 (1961).

[36] J. O. Artman and John C. Murphy, Bull. Am. Phys. Soc. **7**, 14 (1962).

[37] M. G. Cohen and N. Bloembergen, Bull. Am. Phys. Soc. **9**, 88 (1964).

which fitted the ^2E splitting properly, evaluated $2D$ as -0.16 cm^{-1} as compared to the experimental -0.38 cm^{-1} value. These authors suggest that configuration mixing is important when computing the finer spectral details. A proposal by Kamimura,[38] which involves considerations of trigonal field and anisotropic spin-orbit effects, as in the former analysis[2] makes the relation between the $^4A_2$ and ^2E splittings less direct. The pressure dependences of the ground-state splitting and the ^2E splitting are markedly different, but as discussed later, the complexity of these higher order effects makes any interpretation difficult.

We have suggested[29,31] that in view of the comparatively large MEE, a significant contribution to $2D$ could arise from the odd crystal fields. Neglecting the small V_{X2} and V_{XA} values, we expected that $2D \simeq$MEE $\times\frac{1}{2}V_{X1}/V_A$. A value of -0.27 cm^{-1} is thus obtained. However, experimentally the ground-state splittings for the isoelectronic sequence Mn^{4+}, Cr^{3+}, and V^{2+} are about the same [-0.39 (Ref. 39), -0.38 (Ref. 40) and -0.33 (Refs. 41, 42) cm^{-1}, respectively] although properties such as R line fluorescent lifetimes[39,42] and OEE values[34,43] are significantly different. A possible explanation for this paradox is suggested from the ruby optical intensity analyses made earlier in this paper. We recollect that the $(t_1\|V_{X1}\|e)$ matrix element was found to be small compared to the $(t_1\|V_{X1}\|t_2)$ matrix element since in the former the r^1 and r^3 components of V_{X1} subtract whereas in the latter they add algebraically. A MEE perturbation loop of the form

$$^4A_2(V \text{ spin-orbit}) \rightarrow {}^4T_2(V \text{ applied}) \rightarrow {}^4\Gamma_u(V \text{ spin-orbit}) \rightarrow {}^4\Gamma_{u'}(V_{X1}) \rightarrow {}^4A_2$$

would contain $(t_1\|V(\text{applied})\|e)$ and $(t_1\|V_{X1}\|t_2)$. Replacement of V(applied) by V_{X1}, which is permissible since they both belong to the same group representation, would then produce only a *small* contribution to $2D$. Hence in retrospect our previous conclusion, that a large MEE implies a large odd-field contribution to $2D$, is not necessarily valid.

EFFECTS OF PRESSURE ON THE OPTICAL AND MICROWAVE SPECTRA OF RUBY

The effect of stress (parallel and normal to the c axis) on the R lines has been investigated by Schawlow[44] and also by Kaplianskiĭ and Przhevuskiĭ.[45] Hydrostatic pressure experiments on the broad optical bands were performed by Stephens and Drickamer.[46] Earlier R line hydrostatic results appear in the work of Paetzold.[47] We associate the major contribution to the band energies with $10Dq$. The band splittings (and also the R line splittings) are proportional to v. Because of the different radial dependences of the lattice sums, we expect the band energies to be much more sensitive to pressure than the R line differences.

The logarithmic variation of $10Dq$ with hydrostatic pressure is

$$\left(\frac{1}{P}\right)\frac{\delta(10Dq)}{(10Dq)}=5\left[S_{11}+S_{12}+S_{13}+\frac{(S_{13}+S_{33}-S_{11}-S_{12})(6.4B_5^{3*}+0.1404B_5^{0*})}{B_4^3+0.1404B_4^0}\right]. \quad (11)$$

Dipole contributions to $\delta(10Dq)$ have not been included since they are very small. The contribution involving the B^* is present because of the nonisotropic nature of the lattice. The variation of the trigonal field v with pressure along the c axis is

$$(1/P)\delta v/v=\{[3B_2^0+(14.820B_4^0-0.5240B_4^3)\langle r^4\rangle/\langle r^2\rangle]\rho + [3B_3^{0*}+(14.820B_5^{0*}-3.354B_5^{3*})\langle r^4\rangle/\langle r^2\rangle](1-\rho)\} \times S_{33}/N, \quad (12)$$

$$N=B_2^0+(2.964B_4^0-0.1048B_4^3)\langle r^4\rangle/\langle r^2\rangle,$$

$$\rho=S_{13}/S_{33}.$$

For hydrostatic pressures below 6×10^{10} dyn/cm^2 Stephens and Drickamer[46] found no measurable variation in v as inferred from behavior of the band separations (above this pressure nonlinear effects appear). They did find $10Dq$ to vary as R^{-5} as expected from the monopolar model. (Similar results were obtained for Ti^{3+}, V^{3+}, Ni^{2+}, and Ni^{3+} ions in corundum.[48]) Since, it will be recollected that dipole contributions to $10Dq$ were small, this is just as expected. In addition, the term involving the B's and B^*'s amounts only to 0.053 of the "isotropic" term in (11). At 3×10^{10} dyn/cm^2 our formula predicts a $\delta(10Dq)/(10Dq)$ of 1.99×10^{-3}; Drickamer found a value of 1.76×10^{-3}, 12% below our value.

[38] H. Kamimura, Phys. Rev. **128**, 1077 (1962).
[39] S. Geschwind, P. Kisliuk, M. P. Klein, J. P. Remeika, and D. L. Wood, Phys. Rev. **126**, 1684 (1962); Ref. 29, p. 113.
[40] A. A. Manenkov and A. M. Prokhorov, Zh. Eksperim. i Teor. Fiz. **28**, 762 (1955) [English transl.: Soviet Phys.—JETP **1**, 611 (1955)].
[41] J. Lambe and C. Kikuchi, Phys. Rev. **118**, 71 (1960).
[42] M. D. Sturge, Phys. Rev. **130**, 639 (1963).
[43] M. D. Sturge and K. A. Ingersoll, Bull. Am. Phys. Soc. **8**, 215 (1963); M. D. Sturge, Phys. Rev. **133**, A795 (1964).
[44] A. L. Schawlow, *Advances in Quantum Electronics*, edited by J. R. Singer (Columbia University Press, New York, 1961), p. 50.
[45] A. A. Kaplianskiĭ and A. K. Przhevuskiĭ, Dokl. Akad. Nauk SSSR **142**, 313 (1962) [English transl.: Soviet Phys.—Doklady **7**, 37 (1962)].
[46] D. R. Stephens and H. G. Drickamer, J. Chem. Phys. **35**, 427 (1961).
[47] H. K. Paetzold, Z. Physik **129**, 123 (1951).
[48] S. Minomura and H. G. Drickamer, J. Chem. Phys. **35**, 903 (1961); see also the article by Drickamer, in *Solids Under Pressure*, edited by W. Paul and D. M. Warschauer (McGraw-Hill Book Company, Inc., New York, 1963), p. 357.

According to theory,[28] the R line splitting (R_2-R_1) equals $\frac{4}{3}v\zeta/[W(^2T_2)-W(^2E)]$, where ζ denotes the spin-orbit factor. Schawlow's result for stress along the c axis is $(1/P)\delta(R_2-R_1)/(R_2-R_1)=-1.83\times10^{-12}$ cm²/dyn. He found the relative change in R line frequency for perpendicular stress to be -0.65 the parallel result. The data of Kaplianskiĭ and Przhevuskiĭ are similar. (This sign reversal is reminiscent of the Al^{3+} quadrupole pressure results.) The hydrostatic R line pressure variations predicted from these experiments are small, in reasonable agreement with Paetzold's data and in accord with Drickamer's inability to observe a variation in v from the optical band data. In Eq. (12) for $\delta v/v$, we find the second term to be dominant. Our computation (including a small correction for dipole contributions) yields $(1/P)\delta v/v=-6.43\times10^{-12}$ cm²/dyn, 3.5 times Schawlow's results. Although Kaplianskiĭ and Przhevuskiĭ assert that they have also measured the pressure behavior of the $^2T_2$ level, they give no quantitative data; hence, we are unable to estimate the contribution of the energy denominator to variations of (R_2-R_1). The spin-orbit factor ζ might be expected to increase with pressure, making the net result less negative.

The effects of c-axis stress on the $^4A_2$ ground-state microwave splitting $2D$ have been investigated by Watkins and Tucker,[49] and Donoho and Hemphill[50] among others. Their data correspond to a $(1/P)\delta D/D$ value of 1.0×10^{-11} cm²/dyn. Clark, Sands, and Kikuchi[51] have recently reported a hydrostatic result corresponding to $(1/P)\delta D/D$ equalling 1.79×10^{-12} cm²/dyn. Although the $\delta v/v$ computation -6.43×10^{-12} of Eq. (12) did fit the R line data roughly, it is in very poor agreement with the Watkins[49] and Donoho[50] experiments. We also have computed the hydrostatic pressure value of $(1/P)\delta v/v$ finding -3×10^{-13} cm²/dyn, which contrasts strongly with the Clark result.[51]

A c-axis stress formula for δv based on the V_{X1} type odd fields yielded -5×10^{-13}. Additional computations which were made suggest that stress changes in the crystallographic position parameters w and v could affect lower order sums such as those of Eq. (12) much more than the higher order sums, Eq. (11). As indicated earlier such shifts in w and v could easily escape detection by x-radiation analysis. In conclusion it seems clear that the complicated higher order perturbation nature of the ground-state splitting makes the interpretation of stress experiments obscure.

NUCLEAR QUADRUPOLE PARAMETERS FOR Al SUBSTITUENTS IN CORUNDUM

Through the use of electron paramagnetic resonance and electron nuclear double resonance techniques, the quadrupole resonance parameters in corundum of $(Cr^{53})^{3+}$ and the isoelectronic ions $(Mn^{55})^{4+}$ and $(V^{51})^{2+}$ have been determined.[27,52] Although we recognize that quadrupole phenomena are higher order effects which are difficult to calculate, we believe that semiquantitative deductions from our model can help clear up some apparent anomalies.

TABLE XIV. Quadrupole and related data for $(Al^{27})^{3+}$ and its substituents $(Mn^{55})^{4+}$, $(Cr^{53})^{3+}$, and $(V^{51})^{2+}$ in corundum. The order of the R lines in the Mn^{4+} spectrum has not been established.

Nucleus	$(Al^{27})^{3+}$	$(Mn^{55})^{4+}$	$(Cr^{53})^{3+}$	$(V^{51})^{2+}$
Q'(Mc/sec)	0.180(a)	0.138(b)	−0.210(c)	−0.021(b)
I	5/2	5/2	3/2	7/2
Q(barn)	0.149(d)	0.35(e)	0.02(j) −0.03(c)	0.3(f)
$(1-\gamma_\infty)$	3.59(g) 3.31(h)	9.5(i)	10.8(i)	12.7(i)
$q'(\times10^{-13})$	6.4	0.76	−4.54(j)	−0.21
R_2(cm⁻¹)	...	14 786 (k)	14 447 (l)	11 691 (m)
R_1(cm⁻¹)	...	14 866 (k)	14 418 (l)	11 679 (m)
v		?	+	+
Ionic radius(n) (Å)	0.51	0.60	0.63	0.88

[a] From Ref. 13.
[b] From Ref. 52.
[c] From Ref. 27.
[d] From Ref. 16.
[e] From H. Walther, Z. Physik **170**, 507 (1962).
[f] From K. Murakawa and T. Kamei, Phys. Rev. **92**, 325 (1953).
[g] From Ref. 18.
[h] From Ref. 19.
[i] From Ref. 53.
[j] This is the estimate given in the present paper.
[k] From Ref. 39.
[l] From Ref. 28.
[m] From Ref. 42.
[n] *Handbook of Chemistry and Physics*, edited by C. D. Hodgman *et al.* (Chemical Rubber Publishing Company, Cleveland, Ohio, 1962), 44th ed., pp. 3507–3508.

The experimentally measured interaction constant Q' is related to the nuclear electric quadrupole moment Q through the formula $eQ(1-\gamma_\infty)q'=\frac{4}{3}I(2I-1)Q'$, where I is the nuclear spin and q' is $\partial^2V/\partial Z^2$, etc. We would expect on a simple-minded basis a correlation between q' and v (recalling that q' is $4B_2^0$ in our notation) particularly if the B_4 type contributions to v were not too important—as in the case in our ruby model. The value and algebraic sense of v would ordinarily be obtained from band spectra separations. However, if these data were not available, the sign of v can be obtained and the magnitude estimated from the ^2E level (the R line) splittings. We discount in these substituted corunda the traditional immediate relationship between q' and the ground state microwave splitting $2D$. The pertinent data are displayed in Table XIV.

The Q values of Al^{27} of course, Mn^{55}, and V^{51} (but *not* Cr^{53}) are known independently. Terhune *et al.*[27] found the Q' of $(Cr^{53})^{3+}$ to be -0.210 Mc/sec. With Das and Bersohn's value[18] for the $1-\gamma_\infty$ of Al^{3+} and a $1-\gamma_\infty$ estimate of 6 for Cr^{3+}, they then obtained from comparison of the Al and Cr data a Q Cr^{53} value of -0.03 barn. The q' value was assumed to be the same for both ions. They declared their result to be a reasonable one

[49] G. D. Watkins and E. B. Tucker (private communication).
[50] P. L. Donoho and R. B. Hemphill, Bull. Am. Phys. Soc. **7**, 306 (1962); R. B. Hemphill and P. L. Donoho, Bull. Am. Phys. Soc. **8**, 133 (1963).
[51] A. F. Clark, R. H. Sands, and C. Kikuchi, Bull. Am. Phys. Soc. **9**, 36 (1964).
[52] Neal Laurance and John Lambe, Phys. Rev. **132**, 1029 (1963).

TABLE XV. Potential constants for Cr_2O_3, Fe_2O_3, Ti_2O_3, and V_2O_3. Summation over clusters contained within spheres of radius $4A_0$. "Madelung" method.

	Cr_2O_3		Fe_2O_3		Ti_2O_3		V_2O_3	
	nn $\bar{R}=1.99032$	$R=4A_0$ 683 cells	*nn* $\bar{R}=2.02509$	$R=4A_0$ 683 cells	*nn* $\bar{R}=2.04871$	$R=4A_0$ 697 cells	*nn* $\bar{R}=2.01248$	$R=4A_0$ 665 cells
1. B_0^0	43.41330	16.27404	42.70384	16.86588	42.18172	15.02167	42.95408	16.00351
2. B_1^0	−1.64096	0.39593	−1.97945	0.06400	−1.00796	0.98822	−1.01839	0.83778
3. B_2^0	−0.05143	−0.11411	−0.11703	−0.10211	−0.19618	−0.30389	0.00003	−0.05588
4. B_3^0	−0.28281	−0.10678	−0.41230	−0.31596	−0.20163	0.01641	−0.29852	−0.13249
5. B_3^3	−0.50088	−0.43430	−0.76291	−0.67863	−0.40201	−0.35987	−0.51812	−0.46476
6. C_3^3	−0.24869	0.11597	−0.32722	−0.06968	−0.13604	0.19662	−0.16299	0.23096
7. B_4^0	−0.11646	−0.13368	−0.08897	−0.09652	−0.10123	−0.12192	−0.11618	−0.13241
8. B_4^3	−3.64264	−3.48122	−3.24282	−3.09596	−3.27472	−3.13291	−3.52078	−3.35912
9. C_4^3	−0.36347	−0.48182	−0.43295	−0.62392	−0.19689	−0.25348	−0.25005	−0.36076

by suggesting that Cr^{53} (29 neutrons, 24 protons) should on a shell model basis behave similarly to $Cu^{63}(34n,29p)$ and $Cu^{65}(36n,29p)$ with Q values of -0.16 and -0.15, respectively. More recently Laurance and Lambe[52] measured the Q' values for $(Mn^{55})^{4+}$ and $(V^{51})^{2+}$ in corundum and computed Q values using the same q' for all and Sternheimer's Mn^{4+} and V^{2+} antishielding factor evaluations.[53] They arrive at a negative Q for V^{51}, in contrast to the known positive value.

For Cr^{3+} the sign of v and identification of the ^2E levels have been known for some time. V^{2+} has not been observed in absorption since it is overshadowed by the much stronger V^{3+} bands. However, Sturge[42] has made the ^2E level assignments for V^{2+} from Zeeman studies of the excitation spectrum. The order is the same as in ruby. For Mn^{4+} the polarized band absorption data necessary to specify v have not been taken. Although extensive data has been taken on the emission of the R lines,[39] the designation of the ^2E levels has not been made either through polarization or Zeeman studies. (Apparently the crystals are badly strained.) Geschwind[54] believes that the relative intensity of the Mn^{4+} R lines signifies a positive v value—but we consider this still open to question. We do not feel that the existing Mn^{4+} data are sufficient for analysis. The presumption that v is positive, for example, would suggest that q' is negative, contrary to experiment.

As a consequence of the local distortion introduced by Cr^{3+} we had found the Cr^{3+} q' value to reverse sign from the positive Al^{3+} value. If we associate an increase in ionic size with a negative q' tendency, we would expect by extrapolation that $q'(V^{2+})$ be negative (hence v positive). The V^{2+} expectations then would be in accord with the optical and quadrupole experiments. We would expect a similar correlation in ruby using a positive $Q(Cr^{53})$ value. We compute a value of $+0.024$ barn from our monopolar and dipolar sum data. If "covalent" effects are significant in determining the field gradient at the Cr^{3+} and V^{2+} nuclei, we would expect them still to be positive here, opposing and reducing the negative ionic contribution to a smaller value. This could account for the anomalously small field gradient obtained from the V^{2+} resonance and suggest that our computed $Q(Cr^{53})$ value be regarded as a lower bound. We estimate a $Q(Cr^{53})$ upper bound of $+0.05$ barn. (Similar effects may occur in the case of Cu^{3+}.[55]) We recall that, influenced in part by the supposed negative Q, theoreticians have in general had difficulty in predicting other related properties of Cr^{53} such as the nuclear magnetic moment and the magnetic dipole hyperfine-interaction constant.[56,57] In view of these uncertainties we propose that the positive Cr^{53} nuclear electric quadrupole moment suggested by our analysis may provide an independent check of the validity of our model.

SOME OTHER RESULTS FOR CORUNDUM-TYPE STRUCTURES

Table XV presents a compendium of the potential constants for Cr_2O_3, Fe_2O_3, Ti_2O_3, and V_2O_3. The Madelung constants for these lattices were computed to be 24.98, 25.13, 24.87, and 24.97, respectively. In the case of Cr_2O_3 we computed $10Dq$ and v from our tables and formulas using first $\langle r^2\rangle=0.87$, $\langle r^4\rangle=1.68$, the adjusted $B-A$ table values employed earlier in our final ruby calculations. McClure[58] had measured $10Dq=16\,220$ cm^{-1}, $v\approx-700$ cm^{-1}. The monopole sums yielded $10Dq=19\,120$ cm^{-1}, $v=-2101$ cm^{-1}. If we introduce dipoles on the oxygen sites, we find instead $10Dq=18\,679$ cm^{-1}, $v=-1073$ cm^{-1}. Scaling $\langle r^4\rangle$ (and $\langle r^2\rangle$ correspondingly) to match the experimental $10Dq$ value would yield $v=-931$ cm^{-1}. This would represent a multiplication of the original $B-A$ tabulation by 57% instead of the 65% used for ruby.

[53] R. M. Sternheimer, quoted as a private communication in Ref. 52.
[54] S. Geschwind (private communication).
[55] W. E. Blumberg, J. Eisinger, and S. Geschwind, Phys. Rev. 130, 900 (1963).
[56] W. J. Childs, L. S. Goodman, and D. von Ehrenstein, Phys. Rev. 132, 2128 (1963).
[57] K. Ramavataram, Phys. Rev. 132, 2255 (1963).
[58] D. S. McClure, J. Chem. Phys. 38, 2289 (1963).

Similarly, we have computed the odd-field matrix elements. When oxygen dipolar effects are included we find that $(V_{X1})_a=-1.130I_1$, $(V_{X1})_b=-0.318I_3$, $(V_{XA})=-0.1068I_3$, $(V_{X2})=-0.0452I_3$. Except for V_{X2}, these correspond reasonably well to the values we calculated for ruby. McClure[58] found that the Cr bands in Cr_2O_3 were relatively speaking 4.9 times as strong as those in ruby. He has suggested that additional mechanisms for the borrowing of intensity may exist. We had suggested in a previous paper[31] that the ruby electric effect constants might be reduced by one-third when applied to Cr_2O_3 magnetoelectric effect calculations. This conclusion was based in part on the outmoded 0.1 Å McClure ruby model data; dipole lattice sums also had not been considered. Since we now find that the Cr_2O_3 and ruby odd-field lattice sums are about the same, this reduction would appear no longer warranted. In fact, the mechanism responsible for the relative enhancement of the Cr_2O_3 optical spectra might similarly enhance this estimated magnetoelectric effect parameter by a factor of two or so.

We have made a rough computation of $10Dq$ and v for Ti^{3+} in Ti_2O_3 in a manner similar to that of Cr_2O_3. We find these to be 23.5×10^3 cm^{-1} and -4.13×10^3 cm^{-1}, respectively. Inclusion of Ti dipole contributions would be expected to reduce v by about 10%. Blume[59,60] has interpreted Ti_2O_3 neutron diffraction results as corresponding to a v of -200 cm^{-1}. McClure[7] estimated a $10Dq$ and v for Ti^{3+} in Al_2O_3 to be 19.05×10^3 cm^{-1} and 1000 cm^{-1}, respectively. We apparently have a situation here involving reversal in v similar to that for Cr^{3+} in Cr_2O_3 and in ruby. The ionic radius of Ti^{3+} is about 0.25 Å larger than that of Al^{3+}. The distortion occasioned by the insertion of Ti^{3+} in the corundum lattice would be expected to produce a positive value for v.

This section may be an appropriate place to discuss in some detail the results obtained from considerations of the "reduced" Madelung potential.[4] We excise from our X_2O_3 lattice the $(XO_6)^{9-}$ complex formed by an X^{3+} ion and its six nearest O^{2-} neighbors. We then evaluate the (Madelung) potential of the rest of the lattice at various points in the "hole," in particular at the locations of the X ion and of the O ions. For application to ruby and Cr_2O_3 let us consider the standard corundum lattice, the distorted lattice of our ruby model, and the standard Cr_2O_3 lattice. In Al_2O_3 we find the potentials at the Al, upper O, and lower O positions, respectively, to be -27.83688, -27.10290, -29.14119 (in McClure's units, eV per unit charge on the O^{2-} ion per Å) an extreme variation of 7%. Considering -27.10290 as a fiduciary level, these convert to 1.4679, 0, 4.0765 eV or equivalently 1.1840×10^4, 0, 3.2880×10^4 cm^{-1}. For our ruby model we find at the Cr and O positions, -27.71039, -27.07816, -29.21401 or equivalently $1.2770(0.9897\times10^4)$, 0, $4.2842(3.4556\times10^4)$ eV (cm^{-1}). In Cr_2O_3 we find -27.13016, -26.43619, -28.02752 or correspondingly, $1.3879(1.1195\times10^4)$, 0, $3.1826(2.5670\times10^4)$ eV (cm^{-1}). Clearly the potential variation within the hole occupied by the $(XO_6)^{9-}$ complex is well into the frequency region occupied by the optical Cr^{3+} bands. Hence, as indicated earlier, the isolation of the complex from the rest of the lattice does not seem justified on these grounds.

[59] M. Blume (to be published), quoted in Ref. 60.
[60] S. C. Abrahams, Phys. Rev. **130**, 2230 (1963).

SUMMARY

This paper has presented the results of a systematic analysis of the ruby spectrum from an "ionic" point of view. In this case, from the convergence of lattice sums and the failure of the heuristic Sugano-Shulman reduced potential argument,[4] we find that long-range effects contribute importantly to energy level splittings. Hence a calculation restricted to Cr^{3+} and the six nearest oxygen neighbors would be suspect. In view of both the conceptual and computational difficulties associated with a more rigorous treatment, we suggest that the ionic approach is a tractable alternative. Reasonable agreement with many of the properties of ruby system is obtained.

In performing this calculation, particular care was taken in the evaluation of the symmetry adapted lattice sums. We found that direct summation over spheres of increasingly larger diameter does not necessarily lead to rapidly convergent answers. In this connection, we show that the lattice sum convergence is drastically improved by use of a procedure originally suggested for Madelung energy evaluations.[9] The ions are first assembled into chargeless clusters and then a summation over the cluster contributions is effected. In the case of corundum, we select the bipyramidal Al_2O_3 "molecule" as an appropriate cluster. To consider our potential theory in its next approximation we proceed to the explicit evaluation of point dipolar contributions. Here we require the electronic polarizabilities and the electric fields at the various ionic positions. We note that our "Madelung" sum method enables us to compute the requisite electric fields very expeditiously. Although the dipolar contributions to lower order potential terms can be quite substantial, they rapidly become less significant with increasing term order. This is just what one would expect intuitively from a higher order potential distribution approximation.

For application to the Al^{27} electric quadrupole resonance spectrum in corundum, we recomputed the monopolar field gradient and in addition evaluated the dipolar field gradient contribution. Although the dipolar effect is opposite in sign to the monopolar effect, the monopolar effect predominates, contrary to recent assertion.[11] The net calculated field gradient is about 40% of that required by the appropriate formula to match experiment. It has been suggested that "covalent" contributions would supply the remainder.[23] We

have also evaluated the changes of the field gradient with stress predicted by our theory and obtain expressions which agree qualitatively with experiment. We have estimated that the stress-induced changes in the "covalent" contribution are relatively small. We then find reasonable agreement quantitatively between theory and experiment.

In the case of Cr^{3+} in corundum (ruby) we selected four spectroscopic parameters as criteria for judging the validity of our analysis. These were the optical $10Dq$ and v splittings, τ the nearest Al quadrupole resonance frequency enhancement ratio and β the skew angle of the microwave electric effect tensor axes. Although the last two, τ and β, arise from measurement of complex higher order effects, they are sensitive to other aspects of the crystal geometry than $10Dq$ and v. Since τ and β are determined by ratios in which factors extraneous to lattice sums cancel, their interpretation is not as equivocal as might be expected. Unlike the other parameters, β is related rather sensitively to the odd parts of the crystal field.

Perhaps significantly such previous matching efforts involving just $10Dq$ and v as parameters were more flexible in the selection of the geometrical ruby model.[7] We found our situation to be much more restrictive. In particular we were able to obtain a reasonable fit only by distorting the ruby environment in a fashion consistent with what naively might be expected from the data on the disparate Al^{3+} and Cr^{3+} ionic radii. The numerical results were obtained specifically from a model in which 8 ions, the central Cr^{3+} ion, the Al^{3+} immediately below and the two triads of nearest-neighbor oxygens were permitted to move consistent with C_3 symmetry about the Cr—the rest of the lattice remained fixed in the usual positions. In the spirit of our effort the $\langle r^n \rangle$ values used were derived from tables employing Slater-type (hence long-tailed) wave functions. Initially just the monopolar lattice sums were employed. Subsequently dipolar-lattice sums were added, the geometry being maintained as before. Since the Cr^{3+} nearest-neighbor oxygens no longer occupied the standard corundum positions, the orientations and magnitudes of these oxygen dipoles must be changed appropriately. The primary dipolar effect was to double v with smaller changes in β and τ and virtually no change in $10Dq$. Generally the inclusion of dipoles improved the correspondence of our model to experiment.

In this analysis the second-order term was the primary contribution to the trigonal field splitting v; the fourth-order terms occupied a secondary role—this is in direct contrast to an earlier treatment.[7] *A posteriori* we note that the distances between the Cr ion and the nearest neighbor O ions in our ruby model are very close to those in Cr_2O_3, a feature not found in earlier analyses.[7]

Our ruby model was then used in the computation of the odd-field terms necessary for optical intensity and electric effect calculations. The dipolar contribution figured very significantly in some of the lower order odds field sums. The relative intensity values of the band spectra were found to be consistent with our theory. In order to match the absolute intensity to the related optical electric effect value, a C_1 value of 3.8 was required. $[(t_1\|(V_{X1})_a\|e)=C_1(2/3)^{1/2}(t_1\|(V_{X1})_a\|t_2).]$ The internal consistency of our R line optical electric effect calculation required a $\langle\psi_{4p}|z|\psi_{3d}\rangle$ value of 0.43 Å. Although this represents a multiplication of the Ballhausen-Ancmon table result by 3.3 we feel that the value is still small enough to be reasonable. The microwave electric effect in our theory is related to the optical electric effect through a factor h_1 involving spin-orbit energies and optical energy differences. Our revised estimate of h_1 is $\sim 1\times 10^{-3}$. From consideration of the microwave electric effect it could be concluded that odd crystal fields would contribute 70% of the observed ruby microwave $2D$ value. We point out, however, that because of the occurrence of matrix elements involving $(t_1\|V_{X1}\|e)$ rather than $(t_1\|V_{X1}\|t_2)$ this conclusion is not necessarily valid. Moreover, if terms of the form $(t_1\|V(\text{applied})\|e)$ are important in the microwave electric effect, h_1 would be reduced still further by a factor approaching C_1 in value.

The effect of stress on the optical energy difference $10Dq$ is in good accord with the point charge model prediction. The predicted stress variation of v is 3.5 times the effect observed in the ^2E splitting (the R line separation); however, this splitting depends upon other factors as well. Stress variations of the $^4A_2$ ground-state splitting were in poor agreement with expectations based either on variations of the trigonal field v or the V_{X1} odd-field component. A meaningful interpretation of these ground-state results does not seem to be possible at present.

Computations for Cr_2O_3 with ruby radial integral values produced a $10Dq$ value 15% larger than experiment.[58] The sign of v, which is negative in Cr_2O_3, was given correctly. The magnitude of v was in agreement with current rough estimate.[58] The Cr_2O_3 odd crystal field component values were about the same as those of ruby.

Although no calculations similar to the ones presented here were made for other Al substituents, we have attempted to correlate some of the parameters observed in ions isoelectronic to Cr^{3+} with the ruby results. Our conclusion that in ruby the B_4 type contributions to v were negligible suggests a close correlation of v (measured directly from the band splittings or inferred from ^2E level splittings) and the field gradient at the nucleus. Since the ionic radius of V^{2+} is even larger than that of Cr^{3+}, we would expect a similar distortion model to apply. We conclude from our analyses that the observed V^{2+} quadrupole splittings, considered anomalous by others,[52] are consistent with expectations. From a similar analysis applied to ruby we estimate that $Q(Cr^{53})$ (which has not been measured independently) is positive and between 0.02 and 0.05 barn—contrary to the previously proposed negative value.[27]

If we assume that all the odd-field terms scale in the same fashion, a comparison of the Cr^{3+} to the V^{2+} ^2E level fluorescence decay rate suggests a 5 to 1 Cr-V optical electric effect ratio. The observed ratio is 4:1.[43] Consequently from our theory, we would then expect a 4:1 Cr-V microwave electric effect ratio. The V^{2+} microwave electric effect is currently under investigation. Preliminary data[61] yield a Cr-V microwave electric-effect ratio of 2.6 ± 0.5. These data seem to indicate that our "electronic" electric effect model, involving the polarization of the transition metal ion, is adequate to explain both the optical and microwave electric effects.

We have indicated briefly how the behavior of Mn^{4+} is unusual in some respects. We have not attempted to fit this ion with our model. Analyses of some of the pecularities of Mn^{4+} in corundum have appeared elsewhere.[42,43] An anomaly that remains in these substituted corunda is the insensitivity of $2D$ (in magnitude and sign) to the ionic species. We have suggested in this paper that the odd fields responsible for the microwave electric effect need not contribute significantly to $2D$. The microwave splitting then could evolve from more conventional even-parity effects which would not be sensitive to lattice distortion.

After this manuscript was prepared for publication, two recent papers by Macfarlane[62] came to our attention. These develop the parametric dependence of the Cr^{3+} and V^{3+} spectra within the weak field scheme. For ruby, mixing between the approximate strong field (t_2^2e) $^4T_1$ and (t_2^2e) $^4T_2$ configurations gives in this weak field scheme a first-order contribution to the optical band splittings. This effect, which Macfarlane describes in terms of the parameter v', appears in the upper two of the three prominent bands. Two parameters, v and v', are then available to fit the data. The final value of v' obtained (actually from a similar B line calculation[62]) is 650 cm^{-1}; v is evaluated as 800 cm^{-1}. This relatively large v' value indicates that a large departure from strong field coupling certainly exists for the higher bands and possibly also for the (t_2^2e) $^4T_2$ band. For the latter, the first-order effect of v' vanishes in both the weak and strong field schemes. In view of the picture of the relative strength of the crystal field for Cr^{3+} in Al_2O_3 afforded by the conventional E versus Dq/B configuration diagrams, we feel that the value of v' is excessive. Some other explanation for the details of splittings of these upper bands and lines should be sought.

It has been brought to our attention that a forthcoming paper by Moss and Newnham[63] on the determination of the Cr^{3+} position in highly doped ruby through x-radiation techniques. These investigators report that the Cr^{3+} ion in a 4% ruby is shifted 0.06 Å toward the Al below it; i.e., in the opposite sense from the Cr^{3+} shift of the model presented in the present paper. Graham[64] has reported a *uniform* lattice expansion in going progressively from Al to Cr in the solid solution series Al_2O_3–Cr_2O_3. The existence of pairing effects in microwave and optical spectra for Cr^{3+} concentrations substantially below that used by Moss and Newnham has been established. Hence we feel that the relation of these x-ray results to the conclusions of this paper (based on a model pertinent to isolated Cr^{3+} ions) is not clear.

ACKNOWLEDGMENTS

The computations were performed on an IBM 7094 at the Applied Physics Laboratory Computing Center. We are indebted to H. A. Weakliem for a copy of the computing program used by D. S. McClure which was adapted for our purposes by A. L. Bard. The assistance of C. V. Bitterli in this effort is appreciated. Programming in the latter phases of the problem was performed by J. O. A. under the guidance of S. Favin. The illustrations were prepared by A. L. Kozar. We thank Agnes F. Hudson for editorial assistance in the preparation of the manuscript. We express our appreciation to J. J. Krebs for permitting quotation from his preliminary data. We would like to thank M. G. Cohen for pointing out errors in the V_X matrix elements and the neglect of some fractional parentage contributions in the ROEE calculation as they appeared in our earlier paper.[29] We acknowledge continued Bell Systems communications with N. Laurance. We would like to express our appreciation to C. K. Jen for his interest during the course of this research.

[61] James J. Krebs (private communication).
[62] R. M. Macfarlane, J. Chem. Phys. **39**, 3118 (1963); J. Chem. Phys. **40**, 373 (1964).
[63] S. C. Moss and R. E. Newnham, Z. Krist. (to be published).
[64] J. Graham, Phys. Chem. Solids **17**, 18 (1960).